Available online at www.sciencedirect.com
ScienceDirect
Prog. Polym. Sci. 32 (2007) 483–507
PROGRESS IN POLYMER SCIENCE
www.elsevier.com/locate/ppolysci

Mixed matrix membranes (MMMs) comprising organic polymers with dispersed inorganic fillers for gas separation

Tai-Shung Chung[a,*], Lan Ying Jiang[a], Yi Li[a], Santi Kulprathipanja[b]

[a] *Department of Chemical and Biomolecular Engineering, National University of Singapore, 10 Kent Ridge Crescent, Singapore 119260, Singapore*
[b] *UOP LLC, 50 East Algonquin Road, Des Plaines, IL 60017-5016, USA*

Received 16 September 2006; received in revised form 3 January 2007; accepted 16 January 2007
Available online 12 February 2007

Abstract

Gas separation by selective transport through polymeric membranes is one of the fastest growing branches of membrane technology. However, the existing polymeric membrane materials are inadequate to fully exploit the application opportunities on industrial scale; the improvement in permeability is at the expense of selectivity, and vice versa. A new type of membrane material emerging with the potential for future applications is mixed matrix materials composed of homogeneously interpenetrating polymeric and inorganic particle matrices. Compared to original polymeric membranes, significant improvement in separation properties with trivial loss in membrane flexibility is expected for the resultant mixed matrix membranes (MMMs). This review first gives an outline of the concept and the key advances of MMMs. Subsequently, recent developments are presented, including two immediate challenges: achieving an optimized interface structure, and forming asymmetric or composite membrane with an ultrathin and defect-free mixed matrix skin. Attractive avenues to overcome these challenges are emphasized. The review of the Maxwell model demonstrates how the transport properties of MMMs are related to the polymer matrix, molecular sieves, as well as membrane morphology. Finally, future directions of MMMs' fabrication and application are suggested.

Keywords: Mixed matrix membranes (MMMs); Gas separation; Membrane fabrication

Contents

Abbreviations: ABS, acrylonitrile–butadiene–styrene; CA, cellulose acetate; EPDM, ethylene propylene rubber; NBR, nitrile butadiene rubbers; PC, bisphenol-A polycarbonate; PCP, polychloroprene; PEI, polyetherimide; PES, polyethersulfone; PI, polyimide; PMP, poly (4-methyl-2-pentyne); PTMSP, poly (1-trimethylsilyl-1-propyne); PSf, polysulfone; PVAc, polyvinyl acetate; TMHFPSf, tetramethyl hexafluoro polysulfone; 6FDA-IPDA, poly (hexafluoro dianhydride isopropylidene dianiline); 6FDA-MDA, poly (hexafluoro dianhydride methylene dianiline); 6FDA-6FpDA, poly (hexafluoro dianhydride 4, 4′-hexafluoro diamine); 6FDA-6FmDA; poly (hexafluoro dianhydride 3, 3′-hexafluoro diamine)

*Corresponding author. Fax: +65 6779 1936
E-mail address: chencts@nus.edu.sg (T.-S. Chung).

0079-6700/$ - see front matter © 2007 Elsevier Ltd. All rights reserved.
doi:10.1016/j.progpolymsci.2007.01.008

1. Introduction

The separation of gases by membranes is a dynamic and rapidly growing field [1,2]. In membrane-based gas separation process, components are separated from their mixtures by differential permeation through membranes. A number of advantages, including low capital and operating costs, lower energy requirements and, generally, ease of operation are offered by membrane separation [3–8]. As a result, gas separation by membrane process has acquired great significance in the industrial scenario in terms of economical considerations, as gases occupy a central position in the chemical feed stock industry. Current applications of membrane-based gas separation include oxygen and nitrogen enrichment, hydrogen recovery, natural gas separation and the removal of volatile organic compounds from effluent streams [9,10].

The "heart" of a membrane process is the membrane itself. To fully exploit the growing opportunities in the field of gas separation, strong interest exists in the identification of new membrane materials that can comply with current requirements [7]. Criteria for selecting membrane materials for a given separation are complex. Generally, durability, mechanical integrity at the operating conditions, productivity and separation efficiency are important stipulations [6]. Of these requirements, selectivity and permeation rate are the most basic ones. High selectivity and permeability render the operation parameters more flexible (e.g., lower driving force and smaller membrane area to achieve a given separation); therefore, a more efficient separation process results.

In the area of membrane-based gas separation, non-porous polymeric membranes based on solution-diffusion mechanism have been exclusively employed in current commercial devices [11–13]. Typically, polymers have the advantages of desirable mechanical properties and economical processing capabilities. According to the solution-diffusion model, the permeation of molecules through membranes is controlled by two major parameters: diffusivity coefficient (D) and solubility coefficient (S). The diffusivity is a measure of the mobility of individual molecule passing through the voids between the polymeric chains in a membrane material. The solubility coefficient equals the ratio of the dissolved penetrant concentration in the upstream face of the polymer to the upstream penetrant partial pressure. The permeability (P) representing the ability of molecules to pass through a membrane is defined as

$$P = DS. \quad (1)$$

The ability of a membrane to separate two molecules, for example, A and B, is the ratio of their permeabilities, called the membrane selectivity,

$$\alpha_{AB} = P_A/P_B. \quad (2)$$

Since P is the product of D and S, Eq. (2) may be rewritten as

$$\alpha_{AB} = (D_A/D_B)(S_A/S_B). \quad (3)$$

Therefore, the difference in permeability is resulted not only from diffusivity (mobility) difference of the various gas species, but also from difference in the physicochemical interactions of these species with the polymer that determine the amount that can be accommodated per unit volume of the polymer matrix [13,14]. The balance between the solubility selectivity and the diffusivity selectivity determines the selective transport of the component in a feed mixture. Much fundamental research related to the development of polymers with improved gas separation properties focuses on manipulation of penetrant diffusion coefficient via systematic modification of polymer chemical structure or superstructure and either chemical or thermal post-treatment of polymeric membranes [15–22]. Solubility selectivity may also be increased by modifying polymer structure to increase the solubility of one component in a mixture or adding special agents which can complex with a desired penetrant in a mixture [13,23].

Inorganic membranes are usually formed from metals, ceramics, or pyrolyzed carbon [24]. These membranes are increasingly being explored to separate gas mixtures due to the well-known thermal and chemical stabilities and much higher gas fluxes or selectivities as compared to polymeric membranes. Inorganic molecular sieves like zeolites and carbon molecular sieves are excellent materials with diffusivity selectivity significantly higher than polymeric materials. The accurate size and shape discrimination resulting from the narrow pore distribution ensures superior selectivity [25]. Microporous inorganic materials have also been modified to achieve solubility-based separation; in these materials, surface flow and capillary condensation play important roles in increasing the flow of larger species [26]. Early inorganic membranes were developed about 50 years ago [27]. Corning glass developed a homogeneous porous glass (Vycor) with 20–40 Å pores in the 1940s. Also in the 1940s, membranes were developed by the Manhattan Project to enrich uranium by separating uranium isotopes as UF_6. This was the first-large scale gas separation process using inorganic membranes. Membranes of various zeolites with large-pore (*Y*-type [28], *X* [29], *β* [30]), medium-pore (ZSM-5 [31], FER [32]), and small-pore (*A*-type [33], SAPO-34 [34]) are used for gas separation. Some of the membranes have good selectivity. Carbon molecular sieve membranes (CMSMs) are produced by carbonization of a suitable polymeric membrane precursor under controlled conditions. Excellent separation properties of CMSMs have been reported for separation of gas mixtures like natural gas, hydrocarbons, and air [35–37].

2. Concept of mixed matrix membranes (MMMs)

An upper limit for the performance of polymeric membranes in gas separation was predicted by Robeson [38] in early 1990. The performance of various membrane materials available for the separation of O_2/N_2 is depicted in Fig. 1. The figure presents the permeability of the fast gas O_2 on the abscissa on a logarithmic scale and the O_2/N_2 selectivity on the ordinate, again on a logarithmic scale. For the polymeric materials, a rather general trade-off exists between permeability and selectivity,

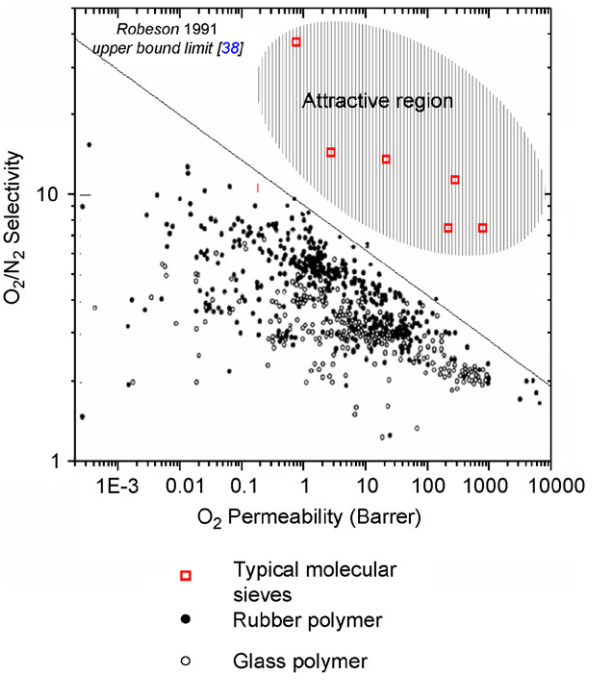

Fig. 1. Relationship between the O_2/N_2 selectivity and O_2 permeability for polymeric membranes and inorganic membranes [38] (the dots indicates the performance of polymeric materials).

with an "upper-bound" evident in Fig. 1. When materials with separation properties near this limit were modified based on the traditional structure–property relation, the resultant polymers have permeability and selectivity tracking along this line instead of exceeding it. On the other hand, as may be seen in Fig. 1, the inorganic materials have properties lying far beyond the upper-bound limit for the organic polymers [39–43]. Though tremendous improvements had been achieved in tailoring polymer structure to enhance separation properties during the last two decades, further progress exceeding the trade-off line seems to present a severe challenge in the near future. Similarly, the immediate application of inorganic membranes is still seriously hindered by the lack of technology to form continuous and defect-free membranes, the extremely high cost for the membrane production, and handling issues (e.g., inherent brittleness) [44,45]. In view of this situation, a new approach is needed to provide an alternate and cost-effective membrane with separation properties well above the upper-bound limit between permeability and selectivity.

The latest membrane morphology emerging with the potential for future applications involves MMM, consisting of organic polymer and inorganic particle phases, as shown schematically in Fig. 2. The bulk phase (phase A) is typically a polymer; the dispersed phase (phase B) represents the inorganic particles, which may be zeolite, carbon molecular sieves, or nano-size particles. MMMs have the potential to achieve higher selectivity, permeability, or both relative to the existing polymeric membranes, resulting from the addition of the inorganic particles with their inherent superior separation characteristics. At the same time, the fragility inherent in the inorganic membranes may be avoided by using a flexible polymer as the continuous matrix.

The investigation of MMMs for gas separation was first reported in 1970s with the discovery of a delayed diffusion time lag effect for CO_2 and CH_4 when adding 5A zeolite into rubbery polymer

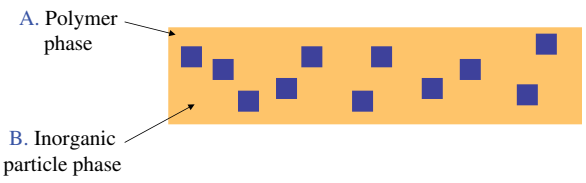

Fig. 2. Schematic of a mixed matrix membrane (MMM).

polydimethyl siloxane (PDMS) [46]. In this work, Paul and Kemp found that the addition of 5A into the polymer matrix caused very large increases in the diffusion time lag but had only minor effects on the steady-state permeation. Researchers at UOP were the first to report that that mixed matrix systems of polymer/adsorbent might yield superior separation performance to that of pure polymeric system [47]. They observed an enhanced O_2/N_2 selectivity from 3.0 to 4.3 when increasing silicalite content in the polymer cellulose acetate (CA) matrix. The concept of MMM has been also demonstrated at UOP LLC in the mid-1980s using CA/silicalite MMMs for CO_2/H_2 separation [48]. In the demonstration, a feed mixture of 50/50 (mol%) CO_2/H_2 with a differential pressure of 50 psi was used. The calculated separation factor for CO_2/H_2 was found to be 5.15 ± 2.2. In contrast, a CO_2/H_2 separation factor of 0.77 ± 0.06 was found for CA membrane. This indicates that silicalite in the membrane phase has reversed the selectivity from H_2 to CO_2.

3. Molecular design and key advances on MMMs

3.1. Conventional MMMs

Much of the research conducted to date on MMM has focused on the addition of porous inorganic filler to polymer matrices. The two materials are required to be selective for the same gas pairs, and, in most case, the inorganic fillers may have selectivity far superior to the neat polymer. Ideally, the incorporation of a small volume fraction of inorganic fillers into the polymer matrix can result in a significant increase in overall separation efficiency, as predicted by the so-called Maxwell model [49]. This model was originally derived for the estimation of the dielectric properties of composite materials [50], but has been widely accepted as a simple and effective tool for estimating MMM properties [49]. The Maxwell model equation for MMMs with dilute suspension of spherical particles can be written as follows:

$$P_{eff} = P_c \left[\frac{P_d + 2P_c - 2\phi_d(P_c - P_d)}{P_d + 2P_c + \phi_d(P_c - P_d)} \right], \quad (4)$$

where P_{eff} is the effective composite membrane permeability, ϕ the volume fraction, P the single component permeability and the subscripts d and c refers to the dispersed and continuous phases, respectively.

To properly choose the dispersed and continuous phases, one must take the transport mechanisms and the gas component preferentially transporting through the membrane into consideration. In some cases, it is more sensible to allow the smaller component to pass through; therefore, inorganic fillers with molecular sieving characteristics and polymers based on the size selection should be combined to produce MMMs. On the other hand, the selective transport of more condensable molecules through the membrane is more economical in some industrial applications. To fulfill this target, the MMMs may include microporous media that favor a selective surface flow mechanism and polymers that separate the mixtures by solubility selectivity [26,51–53]. The MMMs thus produced enable the selective adsorption and/or surface diffusion of more condensable component, while excluding the less condensable component.

Many studies have demonstrated that the remarkable separation properties of MMMs accord with this design, exhibiting performance well beyond the intrinsic properties of the polymer matrix. The most prominent work involved the application 4A zeolite [54–56]. This zeolite has pore a size of 3.8 Å and its O_2/N_2 selectivity at 35 °C is 37, which is much superior to that of glassy polymers [57]. As for polymers more permeable to O_2, the incorporation of 4A zeolite will certainly result in membranes with improved O_2 over N_2 selectivity. Mahajan et al. prepared MMMs containing 4A zeolite in polymers such as polyvinyl acetate (PVAc), Ultem® polyetherimide (PEI), Matrimid® polyimide (PI) among others. With high loadings of zeolites in the polymer matrix, the O_2/N_2 selectivity for MMMs reached almost twice that of pure polymer membranes. Table 1 summarizes the performance of some MMMs developed in this work. Apparently, there exists only trivial difference between the predicted and experimental selectivity. Fig. 3 shows their O_2/N_2 transport properties in comparison with the Robeson, 1991 O_2/N_2 upper-bound limit curve, indicating that MMMs are promising candidates for the next generation of membranes. However, Table 1 also indicates that there is a severe difference in permeability between the model prediction and the experimental values. Clearly, the original Maxwell model should be modified to consider the complexity of MMMs, and this will be taken up in Section 6.

3.2. Unconventional MMMs

Contrary to the aforementioned MMMs consisting of porous fillers and polymeric matrices with similar selectivities, a novel MMM design has been proposed using non-porous nano-size particles [58–60]. The function of the fillers is to systematically manipulate the molecular packing of the polymer chains, hence enhancing the separation properties of glassy polymeric membranes. This approach is partly motivated by the unique transport characteristics of poly (4-methyl-2-pentyne) (PMP), which is a reverse-selective glassy polymer. Because of inherent chain packing characteristics, this material has an intrinsically high free volume. The high free volume reduces the importance of diffusivity selectivity, so that solubility selectivity

Table 1
Mixed matrix membrane performance[a]: predicted vs. observed at 35 °C [54,56]

Polymer	Particle loading (vol%)	Membranes	O_2 permeability[b] (barrier)	O_2/N_2[c] selectivity
	—	Polymeric	0.5	5.9
PVAc [54]	15 vol% loading	MMMs	0.45 (0.53)	7.3–7.6 (7.5)
	25 vol% loading		0.4 (0.55)	8.3–8.5 (8.7)
	40 vol% loading		0.28–0.35 (0.55)	9.7–10.4 (10.9)
Polymer A	—	Polymeric	0.5	7.1
(2,2′-BPDA + BPADA) [54]	20 vol% loading	MMMs	0.47 (0.55)	9.4–9.6 (9.4)
	30 vol% loading		0.4 (0.57)	10.6–10.8 (10.8)
	40 vol% loading		0.37 (0.6)	12.4–12.5 (12.6)
Ultem® PEI [56]	—	Polymeric	0.38	7.8
	15 vol% loading	MMMs	0.38 (0.42)	9.7 (9.7)
	35 vol% loading		0.28(0.49)	12.9 (13.0)

[a]The inorganic phase is zeolite 4A.
[b,c]The data in the parenthesis correspond to Maxwell model prediction.

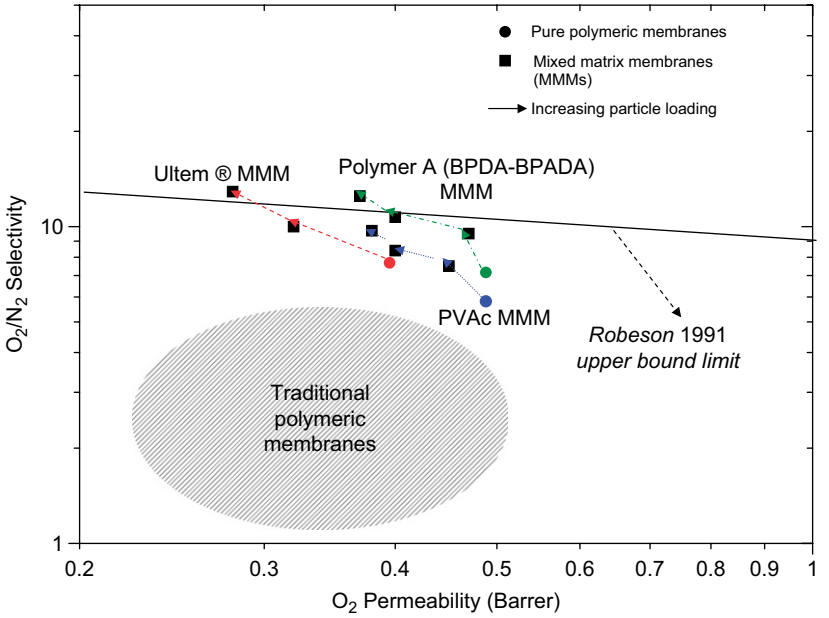

Fig. 3. Mixed matrix membranes performance compared to the Robeson, 1991 upper-bound limit [54,56].

becomes dominant for the overall separation process. As a result, PMP is more permeable to hydrocarbons relative to supercritical gases (e.g., air, nitrogen or methane). Normally, diffusivity selectivity is dominant for gas transport in glassy polymers due to the low mobility of glassy polymer chains, which leads to a faster transport of smaller gas molecules (e.g., H_2) than that of larger gas molecules (e.g., CO_2). However, PMP possesses a high free volume due to its inherent chain packing characteristics. The high free volume may reduce the importance of diffusivity selectivity and make the solubility selectivity dominant for gas transport in PMP membranes. This change in separation mechanism can causes condensable gases (e.g., CO_2) to be more permeable in PMP membranes than non-condensable gases (e.g., H_2), an effect called reverse-selectivity. It is expected that by molecular-level mixing, the nano-size particles with the polymer, the accessible free volume in the polymer matrix might be further increased. The resultant MMM may have separation properties very similar to those of microporous carbons, for which selective surface flow and solubility selectivity prevail [14].

In the work of Merkel et al. [58,60] and He et al. [59], non-porous, nano-size fumed silica, was incorporated into a PMP matrix. Compared to the neat PMP membranes, the selective transport of *n*-butane over methane in the gas mixture obtained with the PMP/fumed silica composite system was

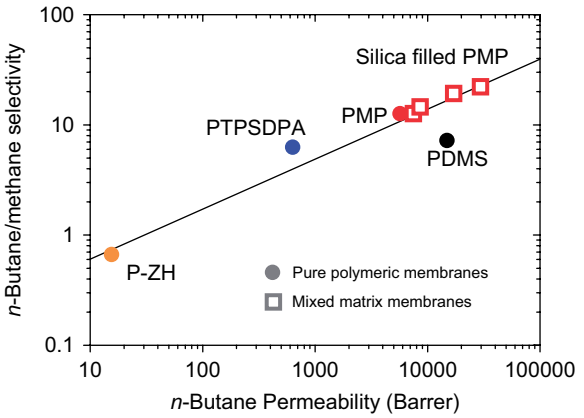

Fig. 4. Mixed gas n-C_4H_{10}/CH_4 selectivity vs. n-C_4H_{10}, permeability for different polymers [59].

tremendously enhanced in both permeability and selectivity. The permeability of this filled system displays a surprising departure from the Maxwell model prediction. Thus, at 50 wt% fumed silica, the PMP/fumed silica nanocomposite's permeability is more than 240% greater than that of neat PMP, whereas the Maxwell's equation predicts a 35% reduction in permeability at the same filler loading. As speculated, the addition of fumed silica particles to PMP has also been confirmed to systematically increase the average size of the free volume. Fig. 4 illustrates the inverse trade-off relationship of *n*-butane/methane selectivity and *n*-butane

permeability for a variety of polymers [59]. The addition of fumed silica in PMP pushes the selectivity and the permeability of the PMP membrane towards a more attractive region with both high selectivity and permeability.

A further example based on the same mechanism was carried out by Merkel et al. [60]. The addition of fumed silica particles to size-selective poly (2,2-bis (trifluoro methyl)-4,5-difluoro-1,3-dioxole-*co*-tetrafluoroethylene) (AF2400) systematically increased penetrant permeability coefficients disrupting the normal chain packing. The enhanced free volume so created weakened the size selectivity to such a degree, that solubility selectivity favoring the hydrocarbon transport dominated the separation process. Therefore, the initially supercritical gas selective membrane was reversed to hydrocarbon selective.

4. Flat dense MMMs

4.1. Recent progress

Flat dense MMMs have been actively pursued in industry and academia for gas separation in the last 20 years. In so far as the MMMs are concerned, the principal improvement in separation properties is expected to capitalize on the positive effect induced by the addition of inorganic phase. Therefore, choosing an inorganic phase suitable for the desired separation is of great significance. Typical inorganic fillers include various zeolites [46–48,54–56,61–76], carbon molecular sieves [61,77–80], activated carbons [81], non-porous silica [58–60,82,83], C_{60} [84], and graphite [68]. The structure properties of the some commonly applied zeolites are summarized in Table 2 [85]. However, due to insufficient information on the separation properties of inorganic fillers in terms of permeability and selectivity, research is often not based on strict design strategies described in Section 3.1, but for exploratory and comparative study. Such properties as filler types [61,63,68], pore size [61,64,66,67], Si/Al ratio [61], cations [61,62,86], pore dimensions [61], and activation temperatures [65] were compared and confirmed to influence the resultant MMM performance. The major systematic work investigating these factors was attributed to Duval [61]. Various silicone rubbers and glassy polymers have been used as the continuous polymeric phase. The general procedure followed by most research to form flat, dense MMM is as follows: (1) preparation of homogeneous polymer/

Table 2
Properties of major zeolite types (adapted from Ref. [85])

Zeolite (examples)	Chemical structure	Si/Al ratio	Pore aperture (Å)	Structure (dimension)	$\rho_{crystal}$ (g/cm^3)	Water sorption (wt%)
LTA (3A, 4A, 5A)	$\{Na_{12}(Al_{12}Si_{12}O_{48})\cdot 27H_2O\}_8$	1	3.2–4.3	3D	1.48–1.69	23
Silicalite-1	Pure silica form of ZSM-5	> 500	5.3*5.6 <–> 5.1*5.5	2D	1.76	1
ZSM-5	$Na_n(Al_nSi_{96-n}O_{192})\cdot \sim 16H_2O$	10–500	5.3*5.6 <–> 5.1*5.5	2D	[a]	4
Faujasite (KY, 13X)	$(Na_2Ca, Mg)_{29}[A_{158}Si_{134}O_{384}]\cdot 240H_2O$	1.5–3	7.4	3D	1.52	26
Theta-1	$Na_n[Al_nSi_{24-n}O_{48}]\cdot \sim 4H_2O$	> 11	4.4*5.5	1D	1.97[b]	[c]
Offretite	$(Ca, Mg)_{1.5}K[Al_4Si_{14}O_{36}]\cdot 14H_2O$	3–4	6.7 <–> 3.6*4.9	3D	1.68	13
Mordenite	$Na_8[Al_8Si_{40}O_{96}]\cdot 24H_2O$	5–5	6.5*7.0 <-> 2.6*5.7	2D	1.82	14

Ref. [85].
[a]Depends on Si/Al ratio.
[b]Calculated for Si/Al ratio = 50.
[c]Unknown.

inorganic filler/solvent mixture, (2) casting the solution on a smooth plate, (3) evaporation of the solvent, and sometimes (4) annealing the membranes at high temperatures to remove the residual solvent. This procedure is quite similar to that of neat dense polymeric membrane formation, which also proves to be an advantage of MMM over the complicated approach adopted in inorganic membrane production. However, it is highly dependent on the polymers, solvents and even particles applied; therefore, no standard procedure has been identified.

The potential for MMMs has been examined for various gas separations, including air separation (e.g., O_2/N_2), natural gas separation (e.g., CO_2/CH_4), hydrogen recovery (e.g., H_2/CO_2, H_2/N_2, and H_2/CH_4), and hydrocarbon separation (e.g., ethylene/ethane, *cis*/*trans*-butylene, *i*-pentane/*n*-pentane, and *n*-butane/CH_4). Studies reporting improved separation efficiency with MMMs are noted in Table 3. Most of the advances in Table 3 were made after 2000. Examination and comparison of these studies reveals that the enhanced molecular sieving is still the major concern when choosing particles and fabricating MMMs [66,70,72,75,82,84]. For CO_2/CH_4 separation, however, the higher condensability and the double bond structure of CO_2 make it possible to utilize other factors (i.e., surface flow or selective adsorption [61,80,81,86]) in increasing the selectivity as suggested in Section 3.

Activated carbon particles have been used as the dispersed phase in an acrylonitrile–butadiene–styrene (ABS) copolymer matrix [82]. The resultant ABS/activated carbon MMMs show a simultaneous increase of CO_2 gas permeabilities (40–600%) and CO_2/CH_4 selectivities (40–100%) over the intrinsic property of ABS membranes. These results could be partially explained considering the existence of a surface flux through the micro–mesoporous carbon media, with a mechanism of preferential surface diffusion of CO_2 over the CH_4 gas. A report by Li et al. [86] is an example on selective sorption. Li et al. proposed a novel exchange treatment of zeolite with noble metal ions, such as Ag^+ and Cu^+, to change the physical and chemical adsorption properties of penetrants in the zeolite. Their data in Fig. 5 show an increase in CO_2 selectivity compared to neat PES membranes and PES/NaA zeolite MMMs. CO_2 can react reversibly with these noble metal ions and form a π-bonded complex, and consequentially, a significantly enhanced CO_2/CH_4 selectivity of around 70% at 40 wt% zeolite loading.

4.2. Variables tailoring MMMs' performance

Among all the studies on MMMs, a number share the view that the performance of MMMs is not a simple addition of the intrinsic properties of individual phase. Many variables may seriously affect MMM performance, making it difficult to understand. Currently, the major concerns in research on MMM are a suitable combination of polymers and particles, the physical properties of the inorganic fillers (e.g., particle size and particle agglomerations), and the polymer/particle interface morphologies.

4.2.1. Suitable combination of polymer/inorganic filler

Even though the selection of appropriate inorganic filler was the major concern in the early development of MMMs, it has been found that the choice of a suitable polymer as the matrix is also important in determining the MMM performance. Examples may be seen in MMMs prepared by Duval [61] with KY zeolite and various silicone rubbers of nitrile butadiene rubbers (NBR), ethylene propylene rubber (EPDM), polychloroprene (PCP), and PDMS. A comparison of the resultant MMMs shows that the intrinsic properties of the original polymers determine the final state of mixed matrix structure; that is, a polymer with low permeability and high selectivity, such as NBR, could result in MMMs with better performance. Similar behavior has been reported by Mahajan and Koros [54,56] on polymer/4A MMMs (refer to Section 3.1). The performance of MMMs with PVAc and Ultem® PEI as the polymer phases reveals that the higher intrinsic selectivity of Ultem® helps it to produce MMMs with superior selectivities in comparison with MMM with PVAc. 5A zeolite has been applied to prepared MMMs along with silicone rubber (e.g., PDMS) [61] or glassy polymers (e.g., polyethersulfone (PES)) [66]; performance enhancement was only observed in the PES/5A system. The poor enhancement in the PDMS/5A system might be due to the extremely slow diffusion of the sorbed gas molecules from the zeolite to the PDMS phase [66].

Therefore, the suitable combination of polymer/inorganic filler is critical for MMM development. The ratio of the resistance presented to the gas transport by the two phases will determine the minimum membrane performance in the absence of defects [87]. When considering a silicone rubber/

Table 3
Major advances of MMCMs

Investigators (year)	Major materials		Major application	Example performance (permeability[a] and selectivity)	
	Polymer	Filler (loading)		Neat polymer	MMMs
Kulprathipanja et al. [47]	CA	Silicalite (25 wt%)	O_2/N_2	—	—
				$\alpha_{O_2/N_2} = 3.0$	$\alpha_{O_2/N_2} = 4.3$
Rojey et al. [76][b]	Ultem® PEI	4A zeolite (19 wt%)	H_2/CH_4	0.35(g/h)H_2 and 0.002(g/h) CH_4 in the permeate side	3.1(g/h) H_2 and 0.0004(g/h) CH_4 in the permeate side
				$\alpha_{CO_2/CH_4} = 14$	$\alpha_{CO_2/CH_4} = 35$
Moaddeb and Koros [82]	6FDA PI	Silica (silica/polymer = 106/8 by weight)	O_2/N_2	—	—
				$\alpha_{O_2/N_2} = 6.9$	$\alpha_{O_2/N_2} = 9.47$
Mahajan and Koros [54]	PVAc	4A zeolite (40 vol%)	O_2/N_2	$P_{O_2} = 0.5$	$P_{O_2} = 0.28\sim0.35$
				$\alpha_{O_2/N_2} = 5.9$	$\alpha_{O_2/N_2} = 9.7\sim10.4$
Wang et al. [72]	Psf	4A zeolite (25 wt%)	O_2/N_2	$P_{O_2} = 1.3$	$P_{O_2} = 1.8$
				$\alpha_{O_2/N_2} = 5.9$	$\alpha_{O_2/N_2} = 7.7$
Guiver et al. [75]	Udel ® Psf	3A zeolite (41 wt%)	H_2/CO_2	$P_{H_2} = 13.9$	$P_{H_2} = 18.2$
				$\alpha_{H_2/CO_2} = 1.6$	$\alpha_{H_2/CO_2} = 13$
Mahajan and Koros [56]	Ultem ® PEI	4A zeolite (35 vol%)	O_2/N_2	$P_{O_2} = 0.38$	$P_{O_2} = 0.28$
				$\alpha_{O_2/N_2} = 7.8$	$\alpha_{O_2/N_2} = 12.9$
He et al. [59], Merkel et al. [58,60]	PMP	Silica (45 wt%)	C_4H_{10}/CH_4	$\alpha_{C_4H_{10}/CH_4} = 13$	$\alpha_{C_4H_{10}/CH_4} = 21$
Chung et al. [84]	Matrimid® PI	C_{60} (10 wt%)	He/N_2	$P_{He} = 25$	$P_{He} = 17$
				$\alpha_{He/N_2} = 87$	$\alpha_{He/N_2} = 106$
Vu et al. [77]	Matrimid® PI	CMS (36 vol%)	CO_2/CH_4	$P_{CO_2} = 10.0$	$P_{CO_2} = 12.6$
				$\alpha_{CO_2/CH_4} = 35.3$	$\alpha_{CO_2/CH_4} = 51.7$
Kulkarni et al. [70][b]	Ultem® PEI	H-SSZ-13 (14 wt%)	O_2/N_2	$P_{O_2} = 0.4$	$P_{O_2} = 0.91\sim0.95$
				$\alpha_{O_2/N_2} = 7.8$	$\alpha_{O_2/N_2} = 10.4\sim10.8$
Anson et al. [81]	ABS	AC (62.4 vol%)	CO_2/CH_4	$P_{CO_2} = 2.5$	$P_{CO_2} = 6.67$
				$\alpha_{CO_2/CH_4} = 24$	$\alpha_{CO_2/CH_4} = 50$
Li et al. [66]	PES	5A zeolite (50 wt%)	O_2/N_2	$P_{O_2} = 0.47$	$P_{O_2} = 0.70$
				$\alpha_{O_2/N_2} = 5.8$	$\alpha_{O_2/N_2} = 7.4$
Li et al. [86]	PES	A zeolite with silver ion exchange (50 wt%)	CO_2/CH_4	$P_{CO_2} = 1.0$	$P_{CO_2} = 1.2$
				$\alpha_{CO_2/CH_4} = 35.3$	$\alpha_{CO_2/CH_4} = 44.0$

[a]Permeability is in unit of Barrer.
[b]Patents.

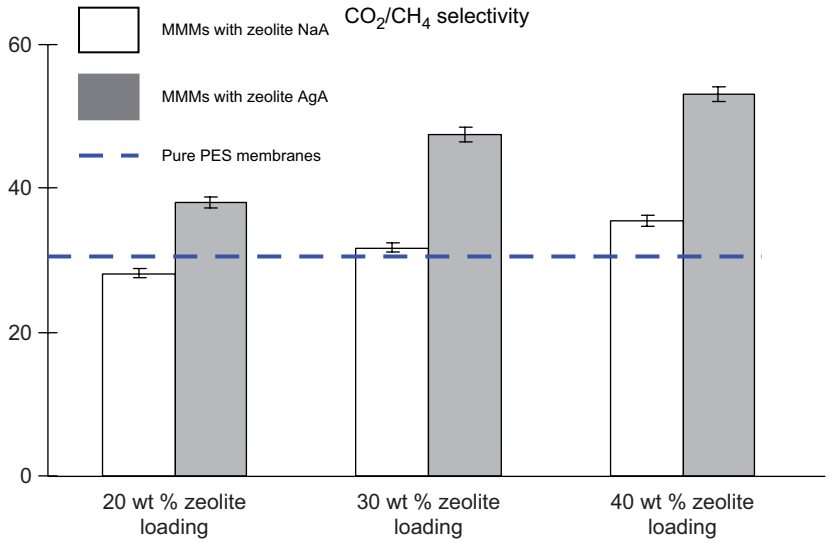

Fig. 5. Comparison of CO_2/CH_4 selectivity of PES–zeolite A MMMs before and after the silver ion (Ag^+) exchange treatment [86].

zeolite MMM, the high permeability and low selectivity of silicone rubber might cause the MMM performance to fall significantly below the upper-bound trade-off curve. The majority of gas diffusion will occur through the phases with lower transport resistance, which is predominantly the silicone rubber phase, instead of the particle phase possibly possessing higher separation performance. Hence, a highly permeable polymer matrix may starve the inorganic porous filler, and make the filler useless. Therefore, the permeability of the polymer matrix and the sieve for the fast gas should be similar.

The aforementioned work is mainly about porous inorganic fillers. The significance of selecting a suitable polymer has also been demonstrated in MMMs containing non-porous fumed silica for *n*-butane/methane separation. Nanoscale fumed silica particles were added inside a series of high free-volume glassy polymers (AF2400, PMP and poly (1-trimethylsilyl-1-propyne (PTMSP)) for the separation of *n*-butane, a condensable gas, from methane, a supercritical gas [58–60,83]. The *n*-butane-selective PMP exhibited significant increase in both permeability and selectivity with the fumed silica addition [58,59]. However, the incorporation of fumed silica converts AF2400 from preferential methane selective to preferential *n*-butane selective [60]. In contrast, the hydrocarbon-selective PTMSP becomes less selective for hydrocarbons with increasing fumed silica loading, as shown in Fig. 6 [83]. The reduction in vapor/permanent gas selectivity for the

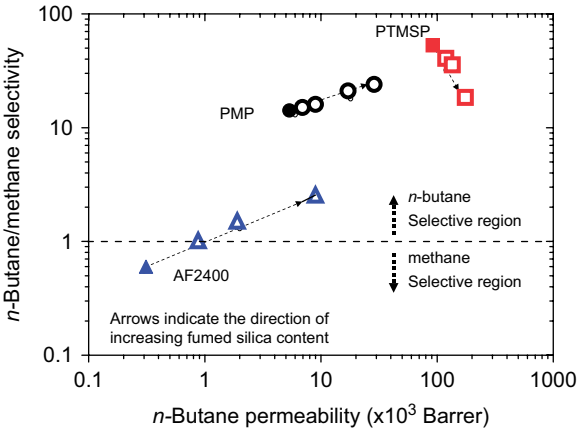

Fig. 6. Mixed-gas *n*-butane/methane permselectivity vs. *n*-butane permeability in: AF2400 and fumed silica-filled AF2400 (18, 30, and 40 wt%); PMP and fumed silica-filled PMP (15, 25, 40, and 45 wt%); PTMSP and fumed silica-filled PTMSP (30, 40, and 50 wt%) [60].

filled PTMSP appears to be related to PTMSP's extremely microporous nature, which, when augmented by fumed silica addition, led to an increasing influence of Knudsen flow.

Generally, Knudsen diffusion dominates the transport mechanism of gases in the porous materials with a pore size of 20 Å smaller. According to Knudsen diffusion, the gas selectivity is inversely proportional to the square root of the diffusant molecular weight [26]. Therefore, the enhanced Knudsen flow in this case made the methane with low molecular weight transport faster than

n-butane. As a result, the initial hydrocarbon selective property was compromised.

4.2.2. Particles size

To date, most of the studies on polymer/inorganic filler MMMs use large particles, with sizes in the micron range. Smaller particles would provide more polymer/particle interfacial area, hence potentially improving the membrane separation performance. In addition, smaller particles are also helpful and essential in the formation of thinner MMMs.

The effect of different particle sizes (0.1, 0.4, 0.7, 0.8, 8.0 μm) of silicalite in PDMS has been investigated [88]. The permeability of MMMs decreases with decreasing particle size of silicalite. This behavior may be due to the enhanced polymer/zeolite interface contact in the case employing relatively smaller particles. The importance of using small filler particles to achieve the desired effect on transport of *n*-butane/methane separation in PMP was demonstrated [59]. At equivalent volume fractions, significant increase in permeability was only observed for particles smaller than 50 nm. It was concluded that smaller particles yield more polymer/particle interfacial area and provide more opportunity to disrupt polymer chain packing and affect molecular transport.

4.2.3. Particle sedimentation and agglomeration

During the fabrication of an MMM, one factor of great importance is particle agglomeration due to sedimentation or migration to the surface. Due to the totally different physical properties and difference in density between zeolite and polymers, precipitation of zeolite may occur during the MMM preparation, resulting in formation of inhomogeneous zeolite and polymer phases in the filled membrane. The agglomeration of zeolites will cause the pinholes that cannot be reached by polymer segments, forming as non-selective defects in the MMM. This situation is especially serious when extending the zeolite loading in the MMM. One solution examined was the preparation of high concentration polymer solutions to increase the viscosity, to slow particle sedimentation [62,89]. Alternatively, one can form the membrane rapidly, so that particles do not have enough time to precipitate [77]. Yet another straightforward, but effective, method is the use of ultra-fine crystallites (<0.5 μm) with a consequent reduction in the sedimentation rate [90]. A more recent example found that good dispersion of fumed silica particles in PMP could be obtained by matching the polarity of the polymer medium and particle surface groups, as well as by controlling film drying conditions [58].

In contrast to sedimentation, particles may move to the membrane surface and agglomerate. This phenomenon often occurs when the membranes are formed at high temperatures. It is believed that agglomeration at the surface is the result of convection cells that form during casting of films [91]. The formation of convection cells in liquids that are heated or cooled can be due to instabilities driven by buoyancy or surface tension (Marangoni effect) [92]. The schematic for the formation of a pattern at the surface is shown in Fig. 7. Increasing casting solution viscosity, decreasing the membrane thickness, and heating the membrane from the top

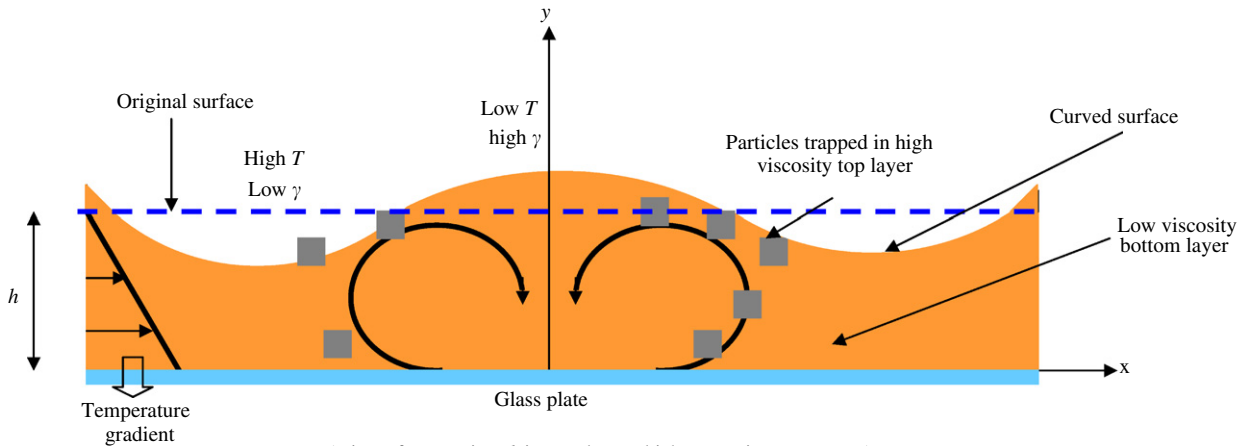

(γ is surface tension; h is membrane thickness; T is temperature)

Fig. 7. Development of the instability in films cast at elevated temperature [91,92].

side may efficiently prevent the surface pattern from propagating.

4.2.4. Interface morphologies

The transport properties of organic/inorganic MMMs are strongly dependent on the nanoscale morphology of the membranes. The morphology of the interface is a critical determinant of the overall transport property. Fig. 8 shows a schematic diagram of various nano-scale structures at the polymer/particle interface. Case 1 represents an ideal morphology, corresponding to the ideal Maxwell model prediction in Eq. (4). Case 2 shows the detachment of polymer chains from the zeolite surface, causing the interface voids. Case 3 indicates that the polymer chains in direct contact with the zeolite surface can be rigidified compared to the bulk polymer chains. Case 4 displays a situation in which the surface pores of the zeolites has been partially sealed by the rigidified polymer chains.

In the first attempt to combine zeolites with a variety of organic polymers, Barrer and James [93] demonstrated that adhesion problems occurred at the polymer/zeolite interface when preparing mixtures of a finely powdered polymer and zeolite crystals. The poor polymer/inorganic filler contact could result in interface voids, presumed to be the major cause for the more or less deteriorated performance as gas molecules take this non-selective and less resistant by-pass instead passing through pores in the particle [61,62,90]. The preparation of zeolite-filled membranes from a glassy polymer by classic dissolution–casting–evaporation was initially investigated by Duval [61]. That process resulted in a three-phase membrane: zeolite, polymer, and interface voids. It was hypothesized that the huge stress occurring during the solvent evaporation step led to dewetting of the polymer from the zeolite external surface. Vankelecom et al. [94] postulated that because of the highly stiff chains of the PI compared to the flexible elastomer, the close packing achieved in the bulk polymer was disturbed in the vicinity of zeolite particles, resulting in voids in the MMM. Other possible causes for the interface voids formation include repulsive force between polymer and filler [89] and different thermal expansion coefficients for polymer and particle [66].

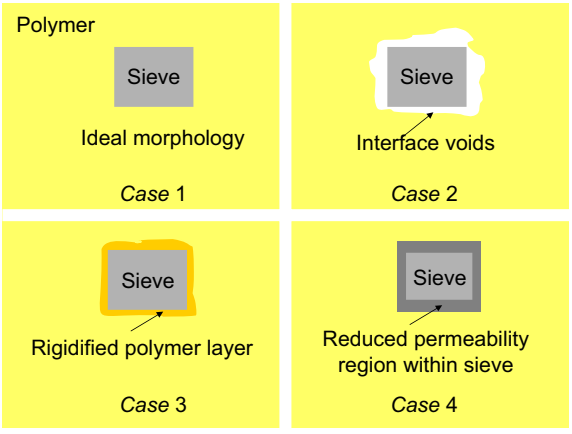

Fig. 8. The schematic diagram of various nanoscale morphology of the mixed matrix structure.

Upon the formation of intimate contact between polymer and particles, other situations including polymer chain rigidification (Case 3) and pore blockage (Case 4) might occur. The mobility of polymer chains in the region directly contacting the particles can be inhibited relative to that for the bulk polymer, an effect called rigidification. Moaddeb and Koros [82] investigated the performance of a series of polymers (poly (hexafluoro dianhydride isopropylidene dianiline) (6FDA-IPDA), poly (hexafluoro dianhydride methylene dianiline) (6FDA-MDA), poly (hexafluoro dianhydride 4,4′-hexafluoro diamine) (6FDA-6FpDA), poly (hexafluoro dianhydride 3,3′-hexafluoro diamine) (6FDA-6FmDA), tetramethyl hexafluoro polysulfone (TMHFPSf), and bisphenol-A polycarbonate (PC)) in the presence of non-porous silicon dioxide particles. The silica particles were brought in close contact with the polymer. Compared to the dense film selectivity of a 6FDA-MDA membrane, increases of as much as 56% in O_2/N_2 selectivity were observed for polymer/silica MMMs. The higher selectivity was attributed to increased rigidity of polymer matrix caused by its adsorption upon the silica surface. Normally, the rigidified polymer region near the particle may have enhanced diffusivity selectivity due to lower mobility of polymer chains; that is, the diffusivity difference between larger and smaller gas molecules may be increased. Consequently, higher selectivity in the vicinity of the particles may be obtained with decreased gas permeability, which contributes to an improvement of overall selectivity of MMMs. A typical characterization to confirm the chain rigidification is glass transition temperature (T_g) analysis. It is widely accepted that T_g may provide a qualitative estimation of the flexibility of polymer chains; therefore, MMMs with polymer chain rigidification have a higher T_g than the original

polymeric membranes [67,77,82,84]. Additionally, an increase in activation energy of permeation may also prove the chain rigidification in the MMMs [82].

For MMMs using porous fillers, pore blockage by the polymer chains (Case 4) in the surface region of porous filler is often evoked [54–56,65,66,68]. Depending on the pore size of inorganic fillers, the polymer chain can fill the pores in various degrees. The zeolite (NaX) could be completely excluded from the transport process as a result of pore filling by the polymer chains; therefore, no improvement in performance could be obtained [68]. On the other hand, the blockage may narrow a part of pores of 5A (4.8 Å) or beta (5.7 × 7.5 Å) zeolites to approximately 4 Å, which can discriminate the gas pair of O_2 and N_2 [66,67]. Since no characterization technique to definitively assess pore blockage is available, it remains an assumption, but see the next paragraph for some qualitative evidence and the discussion in Section 6.

In effect, in MMMs containing porous inorganic fillers, pore blockage is often accompanied by chain rigidification; and there is no experimental design to completely differentiate the influence of these two factors. However, based on the previous research, the following conclusion can be made. Generally, the effects of polymer chain rigidification on the gas separation performance of MMMs are to decrease the gas permeability and increase the gas pair selectivity. Pore blockage of porous fillers always decreases the gas permeability of MMMs, while its effect on the selectivity of MMMs is different when different inorganic fillers are used as the dispersive phase. Pore blockage greatly decreases the selectivity when the original pore size of fillers is comparable to the molecular diameter of the fast gases studied, such as 4A zeolite for O_2/N_2 and CO_2/CH_4 separation, while pore blockage may increase the selectivity when the original pore size of fillers is larger than the molecular diameter of tested slow gases, such as 5A and beta zeolites for O_2/N_2 and CO_2/CH_4 separation. Since chain rigidification only influences a very thin layer (a few μm) of polymer in the vicinity of the particles, any serious decrease of permeability beyond the expectation from chain rigidification may be attributed to pore blockage [66,67,78,89].

With the comprehension of these descriptions about an MMM, it is reasonable to expect some modifications in the Maxwell model, which will be introduced in detail in Section 6. Whatever the polymer/filler combination and mechanism for the improvement of performance might be, the deterioration of the membrane performance by the interface (e.g., defects characterized of Knudsen diffusion) is not desired. Optimization of the interface morphology is the immediate challenges faced by almost all the researches. Till the present, substantial efforts has been made to solve the interface problems. The next section will outline the strategies having the potential to overcome these challenges.

4.3. Optimization of interface morphology

4.3.1. Interface voids

Choosing a polymer with a flexible backbone chain at the membrane formation temperature should significantly suppress dewetting. Silicone rubber generally has a low T_g, and hence is usually flexible at room temperature. This is why it was the most popular polymer in preparing excellent MMMs in most pioneering work. Recently, Pechar et al. [73] proposed the application of a poly (imide siloxane) copolymer, so that the flexible siloxane component provides flexibility and promotes good contact with the zeolite surface. The huge stress induced during the transition from the rubbery state to glassy state as the solvent evaporates with a matrix polymer of a higher T_g is severe, and can pull the polymer chains away from the particle. Therefore, several researchers suggested fabricating or processing an MMM containing glassy polymer at temperatures above T_g [61,62,89]. This suggestion was derived from the observation in MMMs with silicone rubber, because above their usually low T_g, the polymer chains are in a rubbery state and can surround the particles more easily.

An attractive force between the particle and the polymer can be helpful in tailoring the morphology to form an ideal MMM with a perfect interface. A qualitative characterization of the interaction between polymer and sieve was made by Mahajan et al. [91]. The experimental results of atomic force microscopy (AFM) showed that Matrimid®, Ultem®, and PVAc have similarly strong attractive force for the 4A zeolites, while Udel® polysulfone (PSf) has relatively strong repulsive force for the zeolite surface. Gas separation measurements revealed that Matrimid®/4A MMM was defective, while PVAc/4A MMM was superior to the neat PVAc membrane. Recently, activated carbon particles have been used as the dispersed phase in the

ABS copolymer [81]. The intimate interface and the good performance in MMMs were believed to arise from the partial compatibility between styrene–butadiene rubbery chains of ABS copolymer and the activated carbon structure.

In addition to above methods making use of the intrinsic physical properties of the materials, noteworthy work focused on introducing some extra structure to improve the adhesion of the two phases. Silanes coupling agent, an integral chain linker, and surface priming of zeolite have been adopted. The zeolite surface usually has hydroxyl groups; therefore, introducing a group in the polymer chains reacting with hydroxyl group is expected to be effective in preventing interface void formation during the polymer chain shrinkage [91]. The polymer in this work has a T_g of 368 °C. SEM showed excellent contact between polymer and sieve phases. Transport properties of the neat polymer and MMMs indicate improvement with MMMs and a reasonable match between theory and experiment.

In most studies using a coupling agent, amino silane has been chosen. The silane groups can react with the hydroxyl group on the zeolite surface, and the amino groups can react with the some functional groups (e.g., imide group in PI and PEI) in polymers, hence forming covalent bonding between the two phases [61,70,75,89,90,95,96]. Guiver et al. [75] reported PSf/zeolite 3A MMMs. An APTES modified zeolite was covalently attached to aldehyde modified PSf. The H_2/CO_2 selectivity was only 1.6 for the neat PSf membrane, and 3 for PSf/3A MMMs without covalent bonding; while for PSf/3A zeolite MMMs with covalent bonding between the polymer and zeolite, the selectivity was 13. However, it should be kept in mind that the pores of the zeolites should still be available after silylation to fully exhibit their advantages in separation. In this respect, a multilayer deposition of silane may create new voids and should be avoided [95]. Other coupling agents such as benzylamine and 2,4,6-triaminopyrimidine (TAP) have also been proved useful [62,84].

To help promote the polymer/particle interface, a surface priming protocol was suggested by Mahajan [89] in which the particles were coated with an ultrathin layer of the matrix polymer. The resultant MMM with coated 4A zeolite exhibited enhanced selectivity in O_2/N_2 separation compared to the neat PVAc dense film. This priming protocol was further developed by Vu et al. [77] in MMMs containing CMS particles inside Matrimid® or Ultem® films. Enhancement of 40–45% in CO_2/CH_4 selectivity was observed for MMM employing surface priming, but the detailed priming procedure was not disclosed in their study. Recently, Shu et al. [97] identified a novel modification agent (i.e., thionyl chloride) used to create a special zeolite surface morphology having whiskers or asperities. The dramatic increase in the topological roughness on the sieve surface provides enhanced interaction at the polymer/particle interface via induced adsorption and interlocking of polymer chains in the whisker structure. No apparent voids were observed at the sieve–polymer interface by high-resolution SEM. The resultant MMMs all demonstrates improvement in separation efficiency.

Finally, one could also achieve high flexibility during membrane formation with high T_g polymer by the incorporation of a plasticizer (to decrease the T_g) [89]. A rubbery state can be maintained during membrane formation by having the T_g of plasticizer/polymer mixture always below the boiling point of the solvent used in the membrane formation. The resultant MMMs would show improved polymer/sieve interface contact as well as enhanced selectivity for O_2/N_2 gas pair. However, the addition of the plasticizer has changed the polymer matrix separation properties in such a way that they are no longer attractive as the commercial PI.

4.3.2. *Pore blockage and chain rigidification*

Since blockage of the pores by polymer chains may completely eliminate the function of the inorganic filler, investigations are necessary to suppress this effect. Li et al. applied a novel silane coupling agent, (3-aminopropyl)-diethoxymethyl silane (APDEMS) to modify zeolite surface for MMMs [67]; the APDEMS structure and flow chart of this modification process is shown in Fig. 9. The presence of APDEMS introduced a distance of around $(5–9) \times 10^{-10}$ m (5–9 Å) between polymer chains and zeolite surface, thus reducing the extent of the partial pore blockage of zeolites induced by polymer chains. Both gas permeability and gas pair selectivity of PES/A zeolite (APDEMS modified) MMMs are higher than those of PES/zeolite A (not modified) MMMs due to a decrease in the negative effect of partial pore blockage of A zeolite as shown in Fig. 10 [67].

Though chain rigidification has been harnessed to facilitate the selectivity increase [82], it may also seriously depress the permeability, limiting the

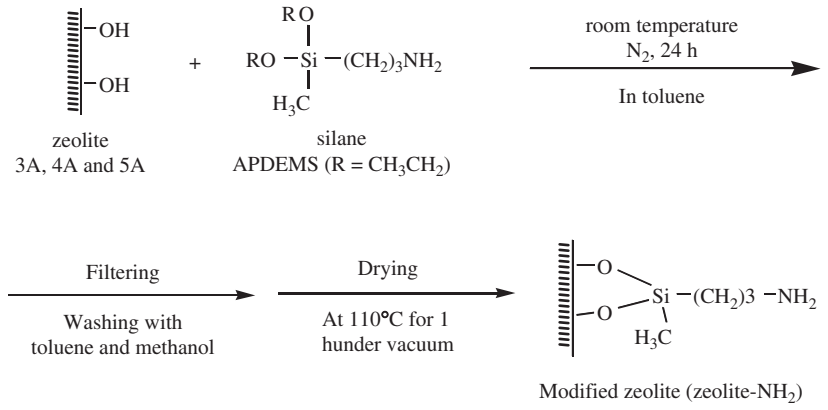

Fig. 9. Flowchart of the chemical modification of zeolite surface [67].

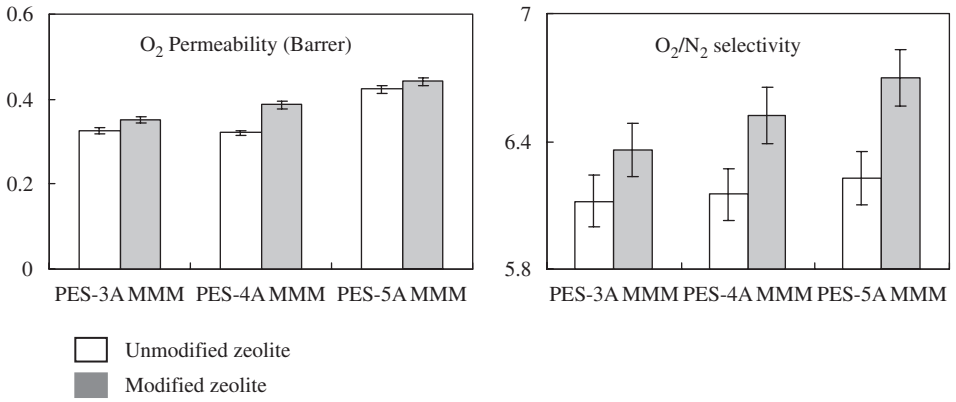

Fig. 10. Comparison of gas permeability and gas pair selectivity of PES–zeolite A MMMs before and after the chemical modification of zeolite surface [67].

usefulness of the MMM. Shu et al. [97] has found a novel zeolite modification agent (i.e., thionyl chloride). When incorporated with the modified zeolites, MMMs of PVAc, Ultem®, and Matrimid® all demonstrated desirable improvement in separation efficiency, parallel to the Maxwell model prediction. The reasonable match between the experimental results and the predictions of the Maxwell model indicates that it may be possible to suppress the undesirable effects of chain rigidification.

5. Asymmetric and composite MMMs

The demand for higher productivity in industrial application necessitates the formation of asymmetric membranes or composite membranes with a thin selective skin on a relatively open-celled porous support to substitute the thicker flat dense membrane. The problem of membrane thickness was first solved by Loeb and Sourirajan [98] with the invention of asymmetric membranes. These membranes had a thin selective skin of approximately 0.2 μm supported by a porous substrate and were applied for reverse osmosis. Usually, only the outer skin layer of the asymmetric membranes performs the gas separation function, while the other portion works as a mechanical supporting substrate. This asymmetric structure was first introduced as the flat sheet membranes, but it was realized that a hollow fiber offers a more practical configuration. The desirable structure of a hollow fiber with a mixed matrix skin is shown in Fig. 11. The highly selective particles are dispersed in the outer skin region of the membranes. While methods to form asymmetric membranes or multilayer composite membranes with an ultrathin mixed matrix selective layer have

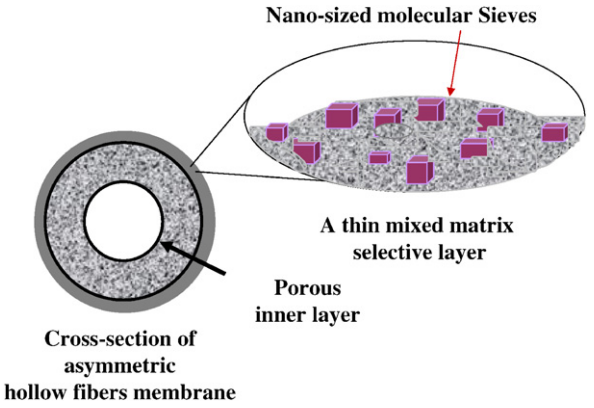

Fig. 11. Schematic cross-section morphology of a hollow fiber with a polymer/zeolite mixed matrix skin.

received a lot of attention, the research in this area is yet quite limited.

5.1. Flat sheet asymmetric MMMs

A flat sheet asymmetric MMM was initially investigated by Kulprathipanja et al. [48]. In their work, the nascent membranes of CA/silicalite formed after partial evaporation were immersed in an ice-water bath; thereafter, the membranes were treated in a hot water bath at 90 °C; finally, the membranes were dried in air. The calculated separation factor for O_2/N_2 for test runs were 3.47, 3.36, and 4.06, all greater than the separation factor of 2.99 for a neat CA membrane. Flat mixed matrix composite membranes were prepared by solution deposition on top of a porous ceramic support by Mahajan [89]. The ceramic supports used were Anodisc membrane filters with a thickness range from 200 to 2000 Å, and offered negligible resistance to gas flow. The membranes were then dried and coated. Individual membrane thickness varied from 5 to 25 μm. However, no separation performance was given. Thin-film zeolite filled PDMS composite membranes, as thin as 3 μm have been prepared by Jia et al. [90]. This thin mixed matrix active layer was produced on top of a porous PEI support by dip coating. Two criteria were essential for the preparation of these membranes: (1) ultrafine particles (0.2–0.5 μm) and (2) prepolymerization of the suspension comprising silicalite, two-component PDMS polymer and *iso*-octane. A slight improvement in separation was only obtained with the membrane having an active mixed matrix layer thickness more than 18 μm.

5.2. Hollow fiber asymmetric MMMs

The most broadly applied technology to form asymmetric hollow fiber membranes is through the phase inversion of a polymer solution. Compared to the mixed matrix flat dense films by cast-evaporation, the formation of integral skinned asymmetric MMMs has the following features: (1) sub-micro-sized particles must be used in order to be fit inside the ultra-thin skin layer, and (2) polymer phase defects and polymer/particle interface defects must be suppressed. Additionally, for asymmetric mixed matrix hollow fiber spinning, a relatively high viscosity dope must be used for spinning to reduce defects [99] and prevent particle sedimentation in the pump during the spinning process. The formation of defects within the polymer phase has been extensively and intensively studied [100–106]. The mechanisms for the formation of interface defects in phase inversion may be the nucleation of non-solvent/polymer lean phase around the inorganic fillers during the phase separation [107], or the effects of an elongation stress during fiber spinning [108].

5.2.1. Hollow fiber asymmetric MMMs by single-layer spinning

An early published work on mixed matrix hollow fibers by phase inversion for gas separation was reported by Bhardwaj et al. [109]. Three different fillers, carbon black, vapor grown carbon fibers, and TiO_2, were incorporated into PSf spinning solutions with the intention of producing highly selective membranes in the form of single-layer hollow fibers with enhanced mechanical strength. The O_2/N_2 selectivity of the 2% w/w carbon black filled membranes was higher than that of the unfilled fibers, while the O_2/N_2 and CO_2/CH_4 selectivity of other filled membranes were lower. Apart from the 5% w/w vapor grown carbon fibers mixed matrix hollow fiber, all the filled membranes exhibited greater mechanical strength (bursting pressure) than the unfilled fibers.

5.2.2. Hollow fiber asymmetric MMMs by dual-layer spinning

Dual-layer co-extrusion technology represents a significant advance in hollow fiber spinning. Fig. 12 gives a schematic diagram of a dual-layer spinneret. Compared to the single-layer asymmetric hollow fibers, the dual-layer hollow fibers by co-extrusion are more attractive for the following advantages: (1)

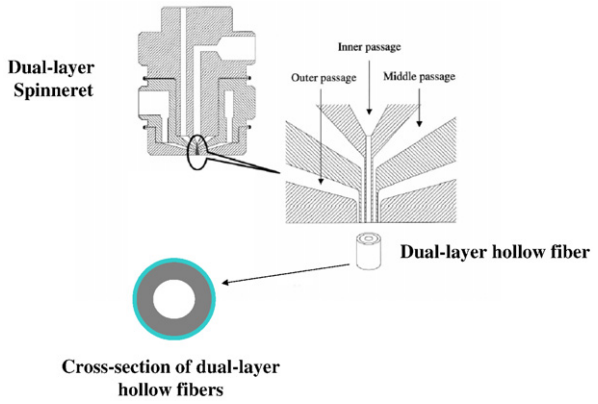

Fig. 12. Schematic of dual-layer hollow fiber spinneret.

the dual-layer fibers can reduce material costs by about 95% or even more, depending on the ratio of the inner layer to outer layer thickness; (2) by means of choosing different materials for the two layer and co-extrusion, it is possible to employ brittle (engineering infeasible), but high performance material as the outer layer to form the composite membrane; (3) by choosing appropriate inner layer and adjusting the dope solution concentration, the porosity in the resultant membrane can be controlled and the dual-layer hollow fibers can withstand high pressures; (4) the simultaneous co-extrusion makes the formation of composite membranes more straightforward and cost-effective compared to other preparation approaches; and (5) higher fluxes can be obtained in the single-step production, since pore penetration, a common problem in the subsequent dip-coating process is avoided [111,112]. The findings in the research on hollow fiber MMMs further add to the attraction of this technology.

The MMM hollow fibers made by Miller et al. [110] from the combination of polyaramide, PI or cellulose with silicalite or ZSM-5 for the separation of *p*-xylene from *p*-xylene/*m*-xylene mixtures. The resultant mixed matrix hollow fibers possessed selectivity for *p*/*m*-xylenes as high as 4, in contrast with about 1 obtained with most polymeric membranes. Hollow fibers having Ultem®/CHA type molecular sieves (pore size 3.8 Å) mixed matrix skins were produced by Ekiner and Kulkarni [113] employing this technology. The resultant hollow fibers had O_2 permeance between 7.4 and 9.5 GPU, and O_2/N_2 selectivity ranging from 8.1 to 8.5. In both patents [110,113], the outer layers containing the selective skin had polymer/particle mixed matrix structures, and the inner layers had neat polymeric structures. As claimed, the application of the dual-layer technology was mainly controlled by the materials cost on the particles. In addition, silane modification of zeolite surface followed by silane linkage to the polymer chains at high temperatures was adopted to improve compatibility between the particle and the polymer. These pioneering studies on hollow fibers with a dense mixed matrix skin were released in patents [110,113,114] without giving much scientific and engineering detail.

Another approach to combat polymer/particle interface defects problem might be the modification of the dispersed particles to increase surface hydrophobicity, leading to a hypothesized suppression of the nucleation of the hydrophilic polymer lean phase around the particles [107].

Unlike the aforementioned studies, a series of studies later contributed by Jiang et al. [115,117] and Li et al. [116] proposed a new approach to produce a defect-free mixed-matrix skin in hollow fibers. In their work, it was found that a skin layer without serious polymer/particle interface voids could hardly be obtained in the traditional phase inversion process [117]. Therefore, the dual-layer co-extrusion technology was applied to control particle distribution and create a situation for subsequently removing defects in the mixed-matrix skin. The materials for the outer layer are the mixed matrix comprising a low T_g glassy polymer (PSf or PES) and nano-size beta zeolite. The polymers for the inner layer are high T_g glassy polymers (Matrimid® and P84®). The vast difference in T_g between the outer and inner layers allows the possibility of performing post-treatment (e.g., heat treatment) to reduce or eliminate the defects in the selective outer layer as well as to eliminate delamination that may exist between the inner and outer layers. When annealing at a temperature above the T_g of the outer layer, the outer layer becomes dense, with much fewer defects due to the release of stress and relaxation of polymer chains in the hollow fibers. A comparison of morphology before and after heat treatment is shown in Fig. 13 [116]. In addition to heat treatment, a new method of *p*-xylenediamine/methanol soaking was employed to obtain an intimate polymer/zeolite interface [117]. In prior studies to remove the interface defects, the zeolite priming process was either carried out before membrane fabrication (e.g., silane modification) or by co-mixing the primer within the casting solutions; while in Jiang et al.'s

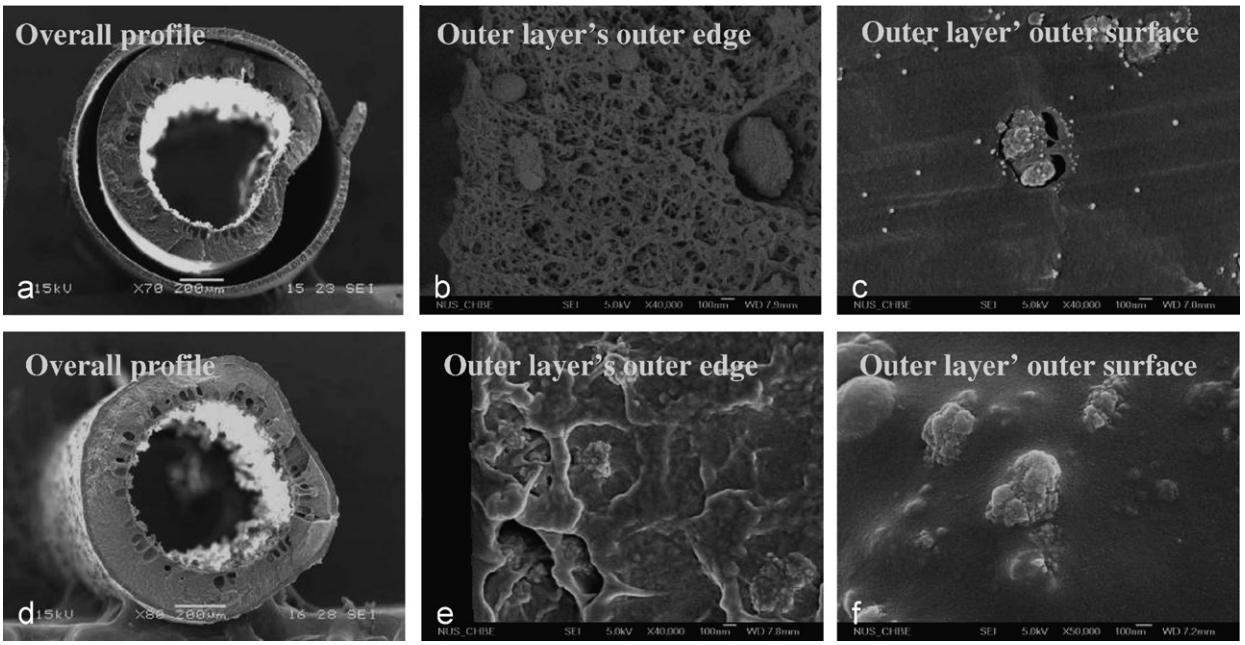

Fig. 13. Comparison of SEM morphologies of dual-layer PES/P84 hollow fiber membranes with a mixed matrix outer layer before and after the heat-treatment (A–C) as-spun hollow fibers; (D–F) hollow fibers heat-treated at 235 °C) [116].

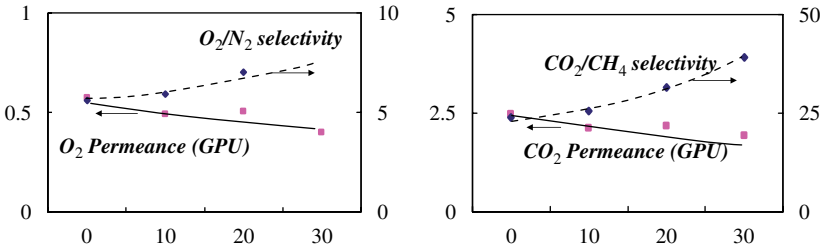

Fig. 14. O_2 permeance and O_2/N_2 selectivity of the dual-layer mixed matrix hollow fibers as a function of zeolite loading after coating: with *p*-xylenediamine/ methanol soaking, heat treated at 200 °C for 2 h. Testing condition: 5 atm, 35 °C.

[117] study, the priming process was performed after hollow fibers formation and solvent exchange. The new procedure may have the advantage of avoiding the agglomeration of nanosize particles caused by the entanglement of the surface modification chemicals, as well as inducing rough zeolite surface, thus reducing chain rigidification. Highly selective mixed matrix hollow fibers for gas separations resulted in these studies. Representative permeance and selectivity in O_2/N_2 and CO_2/CH_4 separation tests are shown in Fig. 14. The ideal selectivities of the mixed matrix hollow fibers with a PSF/beta outer layer (30 wt% of zeolite) and Matrimid® inner layer for O_2/N_2 and CO_2/CH_4 separation were around 30% and 50% superior to that of the neat PSF/Matrimid® hollow fibers, respectively.

5.2.3. *Particle distribution control in hollow fibers*

In a flat sheet MMM, a high particle loading is usually desirable to achieve better separation properties. However, in hollow fiber spinning, an increase in particle loadings may lead to extremely high viscosity, inappropriate for practical fiber spinning. Recent publications by Jiang et al. [108] using nano-size beta zeolite, and Xiao et al. [118] using nano-size TiO_2 suggest the possibility of controlling the particle distribution across the mixed matrix hollow fiber membrane. Based on their observations, the molecular sieve distribution density (or loading) in the polymer matrix of the outer selective skin can be adjusted by the air gap or draw ratio. Their approach provide a much more convenient way of manipulating molecular sieve

distribution and magnifying the effect of molecular sieves in gas separation asymmetric membranes than by simply increasing the molecular sieve loading in the dope solution, since the latter will significantly increase the viscosity of the polymer solution, and cause other problems on spinneret design and spinning process.

6. Modified Maxwell model for performance prediction of MMMs

As has already been noted in Section 3.1, the performance of MMMs can be predicted using the Maxwell model. The Maxwell model was developed in 1873 to predict the permittivity of a dielectric. The constitutive equations governing electrical potential and the flux through membranes are analogs, permitting the application of Maxwell's results to transport in MMMs. The solution to calculate the effective permeability of a MMM with a dilute suspension of spherical particles can be expressed by the well-known Maxwell equation given by Eq. (4), representing an ideal case (no defects and no distortion of the separation properties of the individual phase). This expression must be modified to account for the non-ideal performance of MMMs induced by interface voids, polymer chain rigidification and pore blockage (Section 5, Fig. 8).

Theoretical work on the influence of interface voids (Case 2) in an MMM was first proposed by Mahajan et al. [91] Due to the existence of the interface voids (Fig. 8 Case 2), a three-phase system includes the molecular sieve phase, the polymer phase and the interface voids between these. The permeability P_{3MM} of this three-phase membrane was obtained by applying the Maxwell Model twice.

First, they suggested that gas flow through the interface voids follows Knudsen diffusion, with a slight modification to account for the finite size of the gas molecules:

$$D_{AK} = 9.7 \times 10^{-5} r \sqrt{\frac{T}{M_A}} \left[1 - \frac{d_g}{2r}\right] \tag{5}$$

where D_{AK} is the diffusion coefficient, r the effective pore (defects) radius in Å, T the absolute temperature, M_A the gas molecular weight and d_g is the diameter of the gas molecule in Å. The solution coefficient, S, in these voids is assumed to be the same as in the gas phase and has a partition coefficient taking into considerations the size of the gas molecules relative to the pore radius:

$$S = \frac{1}{\mathrm{RT}} \left(1 - \frac{d_g}{2r}\right)^2 \tag{6}$$

The gas permeability P_I through this interface is the product of D_{AK} and S.

Second, a revised version of the Maxwell equation was used to obtain the permeability of the combined interface void and molecular sieve phase with the interface void as the continuous phase and the molecular sieve phase as the disperse phase:

$$P_{eff} = P_I \left[\frac{P_d + 2P_I - 2\phi_s(P_I - P_d)}{P_d + 2P_I + \phi_s(P_I - P_d)}\right] \tag{7}$$

Here, P_{eff} is the permeability of the combined sieve and interface void, P_d the permeability of the dispersed or sieve phase, P_I the permeability of the interface void, ϕ_d the volume fraction of the sieve phase, ϕ_i the volume fraction of the interface void, and ϕ_s the volume fraction of the sieve phase in the combined phase, given by

$$\phi_s = \frac{\phi_d}{\phi_d + \phi_i}. \tag{8}$$

Finally, the value of the permeability of the combined sieve and interface void, P_{eff}, can then be used along with the continuous polymer phase permeability, P_c, to obtain a predicted permeability P_{3MM} for the three-phase mixed matrix materials by applying the Maxwell equation a second time:

$$P_{3MM} = P_c \left[\frac{P_{eff} + 2P_c - 2(\phi_d + \phi_i)(P_c - P_{eff})}{Pe_{ff} + 2P_c + (\phi_d + \phi_i)(P_c - P_{eff})}\right]. \tag{9}$$

Thus, if one can make an estimate of the volume fraction and the permeability of the interface void region, the Maxwell model can easily be applied to these more complicated morphologies. Where the interface void diameter is large, which is common in MMMs with stiff glassy polymers as the continuous phase, the predicted selectivity by the Maxwell model taking the Knudsen diffusion along the interface void into consideration has never exceeded the selectivity of the neat polymer phase, even though the particles have extremely high selectivity. This predicted phenomenon has been confirmed by the experimental observations [89,90].

The approach in predicting the mixed matrix performance in Case 2 can be readily extended to Case 3 and Case 4, where polymer chain immobilization and permeability reduction in the interface region are used in place of Knudsen diffusion in the

interface voids. The parameters and equations for Case 2–4 are detailed in Table 4 [53,119]. The work on these modified Maxwell models has been summarized in work by Moore and Koros [119], with Ultem® PEI/4A zeolite MMMs as the model system. The predicted and experimental O_2/N_2 selectivity vs. O_2 permeability agreed well each other, which confirms the above mentioned hypotheses. In Mahajan's [89] work, it was found that polymer chain rigidification was dominant over zeolite pore blockage. Recently, the Maxwell model has been further modified by simultaneously considering both zeolite pore blockage and polymer chain rigidification [66,67] as shown in Fig. 15. The Maxwell equation was applied three times in this modified Maxwell model to obtain the final prediction of permeability of MMMs. This modified Maxwell model fitted quite well with the experimental observation, as shown in Fig. 16. A Better fit can be obtained by optimizing each polymer/particle composite system with separate values of the parameters l_i and β.

By applying these modified equations, along with the known intrinsic separation properties of bulk polymer and porous filler, factors leading to non-ideal performance in MMM, such as polymer chain rigidification and pore blockage of inorganic materials, can be estimated quantitatively and in turn, used to help systematically search for methods to offset the negative effects. However, so far only the intrinsic permeability and selectivity of 4A zeolite and CMS for use in O_2/N_2 and CO_2/CH_4 separations were obtained, but these were found to be and relatively consistent with the model [39–43,57]. For other inorganic materials, reliable data cannot be found in the literature because too many experimental conditions may influence the separation properties of inorganic membranes, such as the number of defects on the surface, the type of supporting layer, inorganic membrane thickness, etc. Therefore, quantitative work to match the experimental and predicted results could only be applied to these two materials of 4A zeolite and CMS.

7. Conclusions and perspective

Investigations on MMMs have steadily increased since 1980s when the MMM concept was demonstrated by UOP LLC. Significant experimental results confirm that MMMs show superior separation performance to neat polymeric membranes in

Table 4
Comparison of the modified Maxwell Model for cases 2, 3, and 4 (reprinted from Ref. [119], with permission from Elsevier).

	Case 2	Case 3	Case 4
Parameters	P_I, void permeability	β, chain immobilization factor	β', permeability reduction factor
	$P_I = DS$	$P_I = P_C/\beta$	$P_I = P_C/\beta'$
	$D^a = D_{Knudsen}\left(1 - \frac{\sigma_p}{2r_1}\right)$		
	$S^a = \frac{1}{RT}\left(1 - \frac{\sigma_p}{2r_1}\right)$		
	l_φ, void thickness	l_I, thickness of rigidified region	l_φ, thickness of the reduced permeability region
Model for the pseudo-dispersed phase permeability	$P_{eff} = P_I\left[\frac{P_d + 2P_I - 2\phi_s(P_I - P_d)}{P_d + 2P_I + \phi_s(P_I - P_d)}\right]$	$\phi_s = \frac{\phi_d}{\phi_d + \phi_i} = \frac{r_d^3}{(r_d + l_i)^3}$ or $\frac{(r_d + l_i)^3}{r_d^3} l_i = l_I, l_\varphi$ or $l_{\varphi'}$	
Pseudo-dispersed phase components	Zeolite + surrounding voids	Zeolite + surrounding polymer of reduced permeability	Zeolite (including bulk zeolite and region of reduced permeability)
Model for the overall mixed matrix material		$P_{3MM} = P_c\left[\frac{P_{eff} + 2P_c - 2(\phi_d + \phi_i)(P_c - P_{eff})}{P_{eff} + 2P_c + (\phi_d + \phi_i)(P_c - P_{eff})}\right]$	

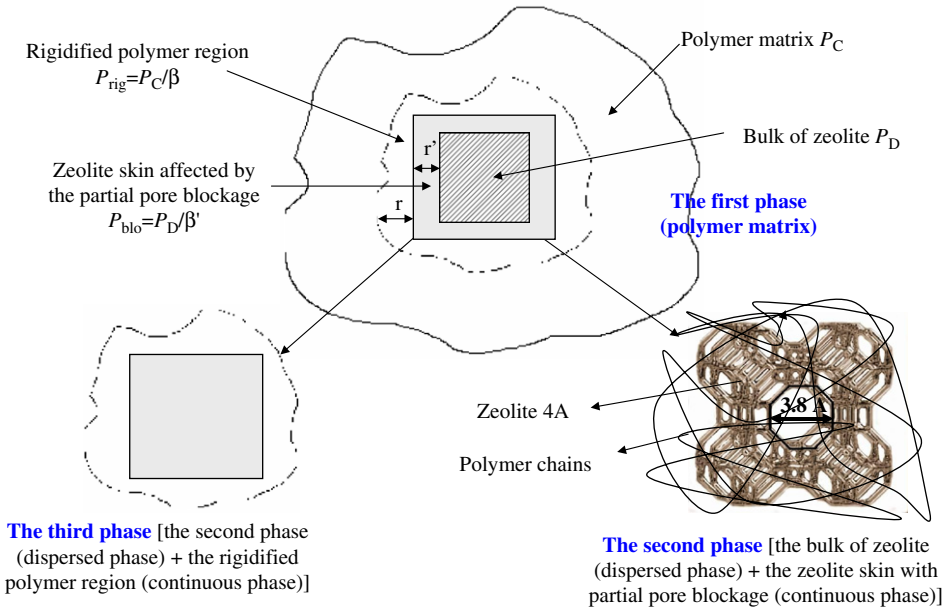

Fig. 15. Schematic diagram for the modified Maxwell model simultaneously considering both zeolite pore blockage and polymer chain rigidification [67].

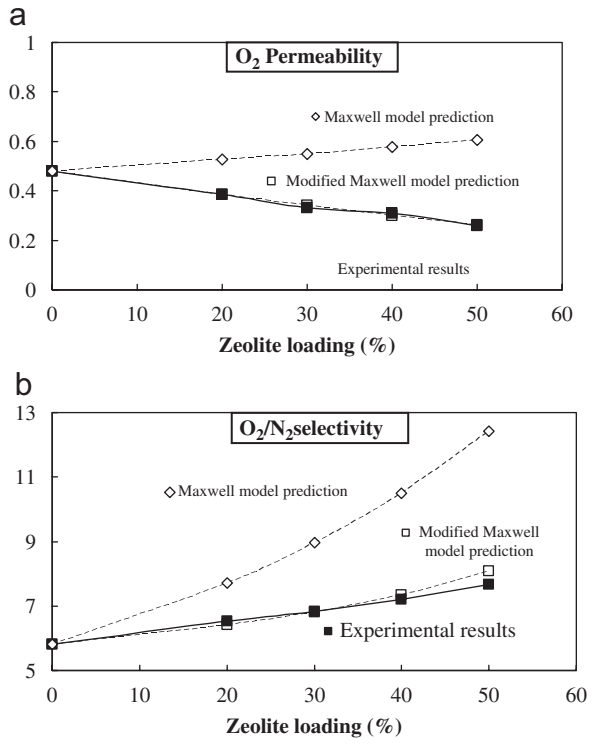

Fig. 16. (A) Comparison of O_2 permeability PES-4A-NH_2 MMMs between experimental data and predictions from the Maxwell model and the modified Maxwell model [67]. (B) Comparison of O_2/N_2 selectivity of PES-4A-NH_2 MMMs between experimental data and predictions from the Maxwell model and the modified Maxwell model [67].

some gas mixtures separation. Clearly, MMMs are promising next-generation membranes for gas separation. However, as may be realized from the preceding review, developments on the fabrication and application of MMMs containing inorganic particles inside polymer matrices for gas separation are still quite low compared those for neat polymeric membranes, providing an opportunity for future developments. For example, it should be noted that successful performance enhancement by mixed matrix concept has been limited to a narrow range of gas separations, summarized in Table 4. In addition, there are few studies on industrially applicable membrane morphology (e.g., asymmetric membranes, thin-film composite membranes). This is mainly due to the lack of sufficient information in the separation properties of membrane materials and fabrication properties of the mixed matrix system.

The keys to the next-generation MMMs may be to produce nano-size fillers less than 20 nm in size, without agglomeration and to obtain their separation properties, especially the porous fillers. A reliable and industrially qualified MMM for a particular separation requires in-depth understanding of separation mechanisms in this hybrid membrane material. The intrinsic properties of the polymer matrix in separation have been well understood using the established technologies. However, the rate of progress in understanding of

inorganic materials falls well behind that of polymer membranes. This makes the material selection a big problem. Therefore, a reliable and standard approach is badly needed to identify the separation properties of inorganic materials.

The complicated situations existing at the interface connecting the polymer and particles make the formation of MMMs with expected performance difficult. The interface defects may make the inorganic particles be isolated from the transport process. The chain immobilization and pore blockage around the interface region could probably lower the permeability. The mechanisms behind these phenomena require intensive investigation. Recent molecular dynamic simulations of mixed matrix materials have shown decreased polymer chain mobility and permeability near an interface [53]. Additionally, molecular dynamic simulation of small penetrants in bulk and confined polymer membranes was performed to understand the effects of confinement on the permeability and selectivity [120]. Changes in the microstructure and dynamics of the polymer were observed upon confinement. With the advances in these works, the effects of particle size and geometry, pore size and geometry, and the polymer/particle interface should also be examined.

Hollow fibers are one of the most efficient membrane morphologies. Nevertheless, research on fabrication of mixed matrix hollow fibers is quite limited. Regarding the different formation mechanisms of dense films from asymmetric membranes, the following aspects should be considered for the formation of defect-free mixed matrix structure in asymmetric membranes: (1) the effect of the rheological properties of the dope solutions and the spinning conditions on skin layer formation, (2) the effect of particle shape and hydrophilicity on the skin layer micro-scale morphology during phase inversion, and (3) a reduction in the skin layer thickness, which entails the employment of ultrafine particles.

As can be concluded in this review, the major gas separations by MMM include air separation and natural gas separation. The investigations on high value-added separations are limited. In the reported studies, the researches on *i*-pentane/*n*-pentane separation, H_2/CO_2 separation, *n*-butane/methane separation paved the way for future work. However, compared to the broad range of separations carried out by neat polymeric membranes, these cases studies are still quite minimal. This indicates that MMM still have a long way to go to fully exploit its potentials.

Acknowledgements

The authors would like to thank A-star, UOP LLC, and NUS for funding this research with the grant numbers of R-398-000-029-305, R-279-000-010-001, and R-279-000-184-112.

References

[1] Rousseau RW. Handbook of separation process technology. New York: Wiley; 1987.
[2] Nunes SPN, Peinemann KV. Membrane technology in the chemical industry. Weinheim, Singapore: Wiley-VCH; 2001.
[3] Berry RI. Membrane separate gas. Chem Eng 1981;88:63–7.
[4] Strathman H. Membrane separation process. J Membr Sci 1981;9:121–89.
[5] Spillman RW, Sherwin MB. Gas separation membranes: the first decade. Chem Technol 1990;20:378–408.
[6] Paul DR, Yampol'skii YP. Polymeric gas separation membranes. Boca Raton, FL: CRC Press; 1994.
[7] Stern SA. Polymers for gas separations: the next decade. J Membr Sci 1994;94:1–65.
[8] Mulder M. Basic principles of membrane technology. Dordrecht: Kluwer Academic Publisher; 1996.
[9] Ho WSW, Sirkar KK. Membrane handbook. New York: Van Nostrand Reinhold; 1992.
[10] Kesting RE, Fritzsche AK. Polymeric gas separation membranes. New York: Wiley; 1993.
[11] Spillman RW. Economics of gas separation membranes. Chem Eng Prog 1989;85:41–62.
[12] Meindersma GW, Kuczynskyi M. Implementing membrane technology in the process industry: problems and opportunities. J Membr Sci 1996;113:285–92.
[13] Freeman BD, Pinnau I. Polymer membrane for gas and vapor separations: chemistry and material science. Washington, DC: American Chemical Society; 1999.
[14] Freeman BD, Pinnau I. Separation of gases using solubility-selective polymer. Trends Polym Sci 1997;5:167–73.
[15] Pinnau I, Freeman BD. Membrane formation and modification: overview. Washington, DC: American Chemical Society; 1990.
[16] Koros WJ, Flemming GK. Membrane-based gas separation. J Membr Sci 1993;83:1–80.
[17] Bos A, Punt IG, Wessling M, Strathmann H. Plasticization-resistant glassy polyimide membrane for CO_2/CH_4 separations. Sep Purif Technol 1998;14:27–39.
[18] McCaig MS, Paul DR. Effect of UV cross-linking and physical aging on the gas permeability of the thin glassy polyacrylate films. Polymer 1999;40:7209–25.
[19] Bos A, Punt I, Strathmann H, Wessling M. Suppression of gas separation membrane plasticization by homogeneous polymer blending. AIChE J 2001;47:1088–93.

[20] Tin PS, Chung TS, Liu Y, Wang R, Liu SL, Pramoda KP. Effect of cross-linking on gas separation performance of Matrimid membranes. J Membr Sci 2003;225:77–90.
[21] Shao L, Chung TS, Hong GH, Pramoda KP. Polyimide modification by a linear aliphatic diamine to enhanced transport performance and plasticization resistance. J Membr Sci 2005;256:46–56.
[22] Chung TS, Shao L, Tin PS. Surface modification of polyimide membranes by diamines for H_2 and CO_2 separation. Macromol Rapid Commun 2006;27:998–1003.
[23] Morisato A, He Z, Pinnau I, Merkel TC. Transport properties of PA 12-PTMO/AgBF4 solid polymer electrolyte membranes for olefin/paraffin separation. Desalination 2002;145:347–51.
[24] Morooka S, Kusakabe K. Microporous inorganic membranes for gas separation. MRS Bull 1999;24:25–9.
[25] Koresh JE, Soffer A. Study of molecular sieve carbons. Part 2. Estimation of cross-sectional diameters of non-spherical molecules. J Chem Soc Faraday I 1980;76: 2472–80.
[26] Rao MB, Sircar S. Performance and pore characterization of nanoporous carbon membranes for gas separation. J Membr Sci 1996;110:109–18.
[27] Pandy P, Chauhan RS. Membranes for gas separation. Prog Polym Sci 2001;26:853–93.
[28] Kusakabe K, Kuroda T, Morooka S. Separation of carbon dioxide from nitrogen using ion-exchanged faujasite-type zeolite membranes formed on porous support tubes. J Membr Sci 1998;148:13–23.
[29] Kita H, Fuchida K, Horita T, Asamura H, Okamoto K. Preparation of faujasite membranes and their permeation properties. Sep Purif Technol 2001;25:261–8.
[30] Tuan VA, Li S, Falconer JL, Noble RD. In situ crystallization of beta zeolite membranes and their permeation and separation properties. Chem Mater 2002;14:489–92.
[31] Yan Y, Davis ME, Gavalas GR. Preparation of zeolite ZSM-5 membranes by in situ crystallization on porous Al_2O_3. Ind Eng Chem Res 1995;34:1652–61.
[32] Nishiyama N, Ueyama K, Matsukata M. Synthesis of FER membrane on an alumina support and its separation properties. Stud Surf Sci Catal 1997;105:2195–205.
[33] Aoki K, Kusakabe K, Morooka S. Gas permeation properties of A-type zeolite membranes formed on porous substrate by hydrothermal synthesis. J Membr Sci 1998; 141:197–209.
[34] Li S, Falconer JL, Noble RD. SAPO-34 membranes for CO_2/CH_4 separation. J Membr Sci 2004;241:121–35.
[35] Vu DQ, Koros WJ, Miller SJ. High pressure CO_2/CH_4 separation using carbon molecular sieve hollow fiber membranes. Ind Eng Chem Res 2002;41:367–80.
[36] Okamoto K, Kawamura S, Yoshino M, Kita H, Hirayama Y, Tanihara N. Olefin/paraffin separation through carbonized membranes derived from an asymmetric polyimide hollow fiber membrane. Ind Eng Chem Res 1999;38: 4424–32.
[37] Xiao YC, Dai Y, Chung TS, Guiver MD. Effects of brominating Matrimid polyimide on the physical and gas transport properties of derived carbon membranes. Macromolecules 2005;38:10042–9.
[38] Robeson LM. Correlation of separation factor versus permeability for polymeric membranes. J Membr Sci 1991; 62:165–85.
[39] Singh AS, Koros WJ. Air separation properties of flat sheet homogeneous pyrolytic carbon membranes. J Membr Sci 2000;174:177–88.
[40] Feuters AB, Centeno TA. Preparation of supported carbon molecular membranes. Carbon 1999;37:679–84.
[41] Kim YK, Lee JM, Park HB, Lee YM. The gas separation properties of carbon molecular sieve membranes derived from polyimides having carboxylic acid groups. J Membr Sci 2004;235:139–46.
[42] Park HB, Kim YK, Lee JM, Lee SY, Lee YM. Relationship between chemical structure of aromatic polyimides and gas permeation properties of their carbon molecular sieve membranes. J Membr Sci 2004;229:117–27.
[43] Tin PS, Chung TS, Kawi S, Guiver MD. Novel approaches to fabricate carbon molecular sieve membranes based on chemical modified and solvent treated polyimides. Micropor Mesopor Mater 2004;73:151–60.
[44] Saracco G, Neomagus HWJP, Versteeg GF, Van Swaaij WPM. High-temperature membrane reactor: potential and problems. Chem Eng Sci 1999;54:1997–2017.
[45] Caro J, Noack M, Kolsch P, Schaefer R. Zeolite membrane-state of their development and perspective. Micropor Mesopor Mater 2000;38:3–24.
[46] Paul DR, Kemp DR. The diffusion time lag in polymer membranes containing adsorptive fillers. J Polym Sci: Polym Phys 1973;41:79–93.
[47] Kulprathipanja S, Neuzil RW, Li NN. Separation of fluids by means of mixed matrix membranes. US patent 4740219, 1988.
[48] Kulprathipanja S, Neuzil RW, Li NN. Separation of gases by means of mixed matrix membranes. US patent 5127925, 1992.
[49] Bouma RHB, Checchetti A, Chidichimo G, Drioli E. Permeation through a heterogeneous membrane: the effect of the dispersed phase. J Membr Sci 1997;128:141–9.
[50] Maxwell JC. Treatise on electricity and magnetism. London: Oxford University Press; 1873.
[51] Anand M, Langsam M, Rao MB, Sircar S. Multicomponent gas separation by selective surface flow (SSF) and polytrimethysilylpropyne (PTMSP) membranes. J Membr Sci 1997;123:17–25.
[52] Sircar S, Rao MB, Thaeron CMA. Selective surface flow membranes for gas separation. Sep Sci Technol 1999;34: 2081–93.
[53] Moore TT, Mahajan R, Vu DQ, Koros WJ. Hybrid membrane materials comprising organic polymers with rigid dispersed phases. AIChE J 2004;50:311–21.
[54] Mahajan R, Koros WJ. Factors controlling successful formation of mixed-matrix gas separation materials. Ind Eng Chem Res 2000;39:2692–6.
[55] Mahajan R, Koros WJ. Mixed matrix membrane materials with glassy polymers. Part 1. Polym Eng Sci 2002;42: 1420–31.
[56] Mahajan R, Koros WJ. Mixed matrix membrane materials with glassy polymers. Part 2. Polym Eng Sci 2002;42: 1432–41.
[57] Ruthven DM, Derrah RI. Diffusion of monoatomic and diatomic gases in 4A and 5A zeolites. J Chem Soc: Faraday Trans 1975;71:2031–7.
[58] Merkel TC, Freeman BD, Spontak RJ, He Z, Pinnau I. Ultrapermeable, reverse-selective nanocomposite membranes. Science 2002;296:519–22.

[59] He Z, Pinnau I, Morisato A. Nanostructured poly (4-methyl-2-pentyne)/silica hybrid membranes for gas separation. Desalination 2002;146:11–5.
[60] Merkel TC, He Z, Pinnau I, Freeman BD, Meakin P, Hill AJ. Sorption and transport in poly (2,2-bis(trifluoromethyl)-4,5-difluoro-1,3-dioxole-*co*-tetrafluoro-ethylene) containing nanoscale fumed silica. Macromolecules 2003; 36:8406–14.
[61] Duval JM. Adsorbent filled polymeric membranes. PhD thesis. The Netherlands: University of Twente; 1995.
[62] Boom JP. Transport through zeolite filled polymeric membranes. Ph. D. Thesis, The Netherlands: University of Twente; 1994.
[63] Suer MG, Bac N, Yilmaz L. Gas permeation characteristics of polymer–zeolite mixed matrix membranes. J Membr Sci 1994;91:77–86.
[64] Yong HH, Park HC, Kang YS, Won J, Kim WN. Zeolite-filled polyimide membrane containing 2,4,6-triaminopyrimidine. J Membr Sci 2001;188:151–63.
[65] Ersolmaz SBT, Senorkyan L, Kalaonra N, Tatlier M, Senatalar AE. *n*-Pentane/*i*-pentane separation by using zeolite–PDMS mixed matrix membranes. J Membr Sci 2001;189:59–67.
[66] Li Y, Chung TS, Cao C, Kulprathipanja S. The effects of polymer chain rigidification, zeolite pore size and pore blockage on polyethersulfone (PES)–zeolite A mixed matrix membranes. J Membr Sci 2005;260:45–55.
[67] Li Y, Guan HM, Chung TS, Kulprathipanja S. Effects of novel silane modification of zeolite surface on polymer chain rigidification and partial pore blockage in polyethersulfone (PES)–zeolite A mixed matrix membranes. J Membr Sci 2006;275:17–28.
[68] Clarizia G, Algieri C, Drioli E. Filler–polymer combination: a route to modify gas transport properties of a polymeric membrane. Polymer 2004;45:5671–81.
[69] Jia M, Peinemann KV, Behling RD. Molecular sieving effect of the zeolite-filled silicone rubber membranes in gas permeation. J Membr Sci 1991;57:289–92.
[70] Kulkarni SS, David HJ, Corbin DR, Patel AN. Gas separation membrane with organosilicon-treated molecular sieve. US patent 6580860, 2003.
[71] Hasse DJ, Kulkarni SS, Corbin DR, Patel AN. Mixed matrix membranes incorporating chabazite type molecular sieves. US patent 6626980, 2003.
[72] Wang H, Holmberg BA, Yan Y. Homogeneous polymer–zeolites nano composite membranes by incorporating dispersible template-removed zeolite nanoparticles. J Mater Chem 2002;12:3640–3.
[73] Pechar TW, Kim S, Vaughan B, Marand E, Baranauskas V, Riffle J, et al. Preparation and characterization of a poly (imide siloxane) and zeolite L mixed matrix membrane. J Membr Sci 2006;277:210–8.
[74] Pechar TW, Kim S, Vaughan B, Marand E, Tsapatsis M, Jeong HK, et al. Fabrication and characterization of polyimide–zeolite L mixed matrix membranes for gas separation. J Membr Sci 2006;277:195–202.
[75] Guiver MD, Robertson GP, Dai Y, Bilodeau F, Kang YS, Lee KJ, et al. Structural characterization and gas-transport properties of brominated Matrimid polyimide. J Polym Sci: Polym Chem 2003;40:4193–204.
[76] Rojey AR, Deschamps A, Grehier A, Robert E. Process for separation of the constituents of a mixture in the gas phase using a composite membrane. US patent 4925459, 1990.
[77] Vu DQ, Koros WJ, Miller SJ. Mixed matrix membranes using carbon molecular sieves. I. Preparation and experimental results. J Membr Sci 2003;211:311–34.
[78] Vu DQ, Koros WJ, Miller SJ. Mixed matrix membranes using carbon molecular sieves. II. Modeling permeation behavior. J Membr Sci 2003;211:335–48.
[79] Vu DQ, Koros WJ, Miller SJ. Effect of condensable impurity in CO_2/CH_4 gas feeds on performance of mixed matrix membranes using carbon molecular sieves. J Membr Sci 2003;221:233–9.
[80] Duval JM, Folkers B, Mulder MHV, Desgrandchamps G, Smolders CA. Adsorbent filled membranes for gas separation. Part 1. Improvement of the gas separation properties of polymeric membranes by incorporation of microporous adsorbents. J Membr Sci 1993;80:189–98.
[81] Anson M, Marchese J, Garis E, Ochoa N, Pagliero C. ABS copolymer-activated carbon mixed matrix membrane for CO_2/CH_4 separation. J Membr Sci 2004;243:19–28.
[82] Moaddeb M, Koros WJ. Gas transport properties of thin polymeric membranes in the presence of silicon dioxide particles. J Membr Sci 1997;125:143–63.
[83] Merkel TC, He Z, Pinnau I, Freeman BD, Meakin P, Hill AJ. Effect of nanoparticles on gas sorption and transport in poly (1-trimethylsilyl-1-propyne). Macromolecules 2003;36: 6844–55.
[84] Chung TS, Chan SS, Wang R, Lu Z, He C. Characterization of permeability and sorption in Matrimid/C_{60} mixed matrix membranes. J Membr Sci 2003;211:91–9.
[85] Meier WM, Olson DH. Altas of zeolite structure types, 3rd ed. London: Butterworths; 1992.
[86] Li Y, Chung TS, Kulprathipanja S. Novel Ag+-zeolite/polymer mixed matrix membranes with a high CO2/CH4 selectivity. AIChE J 2007;53:610–6.
[87] Zimmerman CM, Singh A, Koros WJ. Tailoring mixed matrix composite membranes for gas separations. J Membr Sci 1997;137:145–54.
[88] Tantekin-Ersolmaz SB. Effect of zeolite particle size on the performance of polymer–zeolite mixed matrix membrane. J Membr Sci 2000;175:285–8.
[89] Mahajan R. Formation, characterization and modeling of mixed matrix membrane materials. PhD thesis. Univeristy of Texas at Austin, 2000.
[90] Jia M, Peinemann KV, Behling RD. Preparation and characterization of thin-film zeolite–PDMS composite membranes. J Membr Sci 1992;73:119–28.
[91] Mahajan R, Burns R, Schaeffer M, Koros WJ. Challenges in forming successful mixed matrix membranes with rigid polymeric materials. J Appl Poly Sci 2002;86:881–90.
[92] Levich VG, Krylov VS. Surface-tension-drive phenomena. Annu Rev Fluid Mech 1969;1:293–316.
[93] Barrer RM, James SD. Electrochemistry of crystal-polymer membranes. I. Resistance measurements. J Phys Chem 1960;64:417–21.
[94] Vankelecom IFJ, Mercks E, Luts M, Uytterhoeven JB. Incorporation of zeolite in polyimide membranes. J Phys Chem 1995;99:13187–92.
[95] Vankelecom IFJ, Broeck SVD, Mercks E, Geerts H, Grobet P, Yutterhoeven JB. Silylation to improve incorporation of zeolites in polyimide films. J Phys Chem 1996;100:3753–8.

[96] Pechar TW, Tspatsis M, Marand E, Davis R. Preparation and characterization of a glassy fluorinated polyimide zeolite-mixed matrix membrane. Desalination 2002;146: 3–9.
[97] Shu S, Husain S, Koros WJ. Formation of nanoscale morphology on zeolite surface for enhanced interfacial interaction in mixed matrix membranes. Chicago, IL: North American Membrane Society; 2006.
[98] Loeb S, Sourirajan S. Sea water demineralization by means of an osmotic membrane. Adv Chem Ser 1962;38: 117–32.
[99] Chung TS, Kafchinski ER, Vora RH. Development of a defect-free 6FDA durene asymmetric hollow fibers and its composite hollow fibers. J Membr Sci 1994;88:21–36.
[100] Pinnau I, Koros WJ. Structures and gas separation properties of asymmetric polysulfone membranes made by dry, wet, and dry/wet phase inversion. J Appl Polym Sci 1991;43:1491–502.
[101] Fritzsche AK, Cruse CA, Kesting RE, Murphy MK. Polysulfone hollow-fiber membranes spun from Lewis acid:base complexes. Part II. The effect of Lewis acid-to-base ratio on membrane structure. J Appl Polym Sci 1990; 39:1949–56.
[102] Kesting RE, Fritzsche AK, Cruse CA, Moore MD. The second-generation polysulfone gas-separation membrane. II. The relationship between sol properties, gel macrovoids, and fiber selectivity. J Appl Polym Sci 1990;40:1575–82.
[103] Cabasso I, Klein E, Smith JK. Polysulfone hollow fibers. II. Morphology. J Appl Polym Sci 1977;21:165–80.
[104] Ekiner OM, Vassilatos G. Polyaramide hollow fibers for hydrogen/methane separation—spinning and properties. J Membr Sci 1990;53:259–73.
[105] Pesek SC, Koros WJ. Aqueous quenched asymmetric polysulfone membranes prepared by dry/wet phase separation. J Membr Sci 1993;81:71–88.
[106] Wang DL, Li K, Teo WK. Polyethersulfone hollow fiber gas separation membranes prepared from NMP/alcohol solvent systems. J Membr Sci 1996;115:85–108.
[107] Husain S, Koros WJ. In mixed matrix hollow fibers for gas separation. Providence, RI: North American Membrane Society; 2005.
[108] Jiang LY, Chung TS, Cao C, Huang Z, Kulprathipanja S. Fundamental understanding of nano-sized zeolite distribution in the formation of the mixed matrix single- and dual-layer asymmetric hollow fiber membranes. J Membr Sci 2005;252:89–100.
[109] Bhardwaj V, Macintosh A, Sharpe ID, Gordeyev SA, Shilton SJ. Polysulfone hollow fiber gas separation membranes filled with submicron particles. Ann NY Acad Sci 2003;984:318–28.
[110] Miller SJ, Munson CL, Kulkarni SS, Hasse DJ. Purification of *p*-xylene using composite mixed matrix membranes. US patent 6500233, 2002.
[111] Jiang LY. Fabrication and characterization of composite membranes for gas separation. PhD thesis. Singapore: National University of Singapore; 2006.
[112] Li Y. Development of mixed matrix membranes for gas separation application. PhD Thesis. Singapore: National University of Singapore; 2006.
[113] Ekiner OM, Kulkarni SS. Process for making hollow fiber mixed matrix membranes. US patent 6663805, 2003.
[114] Koros WJ, Wallace D, Wind JD, Miller SJ, Bickel CS, Vu DQ. Crosslinked and crosslinkable hollow fiber mixed matrix membrane and method of making the same. US patent 6755900, 2004.
[115] Jiang LY, Chung TS, Kulprathipanja S. An investigation to revitalize the separation performance of hollow fibers with a thin mixed matrix composite skin for gas separation. J Membr Sci 2006;276:113–25.
[116] Li Y, Chung TS, Huang Z. Dual-layer polyethersulfone (PES)/BTDA-TDI/MDI co-polyimide (P84) hollow fiber membranes with a submicron PES–zeolite beta mixed matrix dense-selective layer for gas separation. J Membr Sci 2006;277:28–37.
[117] Jiang LY, Chung TS, Kulprathipanja S. A novel approach to fabricate mixed matrix hollow fibers with superior intimate polymer/zeolite interface for gas separation. AIChE J 2006;52:2898–908.
[118] Xiao YC, Wang KY, Chung TS, Tan J. Evolution of nanoparticle distribution during the fabrication of mixed matrix TiO2-polyimide hollow fiber membranes. Chem Eng Sci 2006;61:6228–33.
[119] Moore TT, Koros WJ. Non-ideal effects in organic-inorganic materials for gas separation membranes. J Mol Struct 2005;739:87–98.
[120] Rallabandi PS, Ford DM. Permeation of small molecules through polymers confined in mesoporous media. J Membr Sci 2000;171:239–52.